To Automate Detecting, Quantifying and Mapping of Delamination via Arial Thermography

Zhigang Shen[1], Chongsheng Cheng[1], Ri Na[2], Zhexiong Shang[1]

[1]Durham School of Architectural Engineering and Construction

113 Nebraska Hall, University of Nebraska – Lincoln

[2]Department of Civil and Environmental Engineering

342B DuPont Hall, University of Delaware

FINAL REPORT

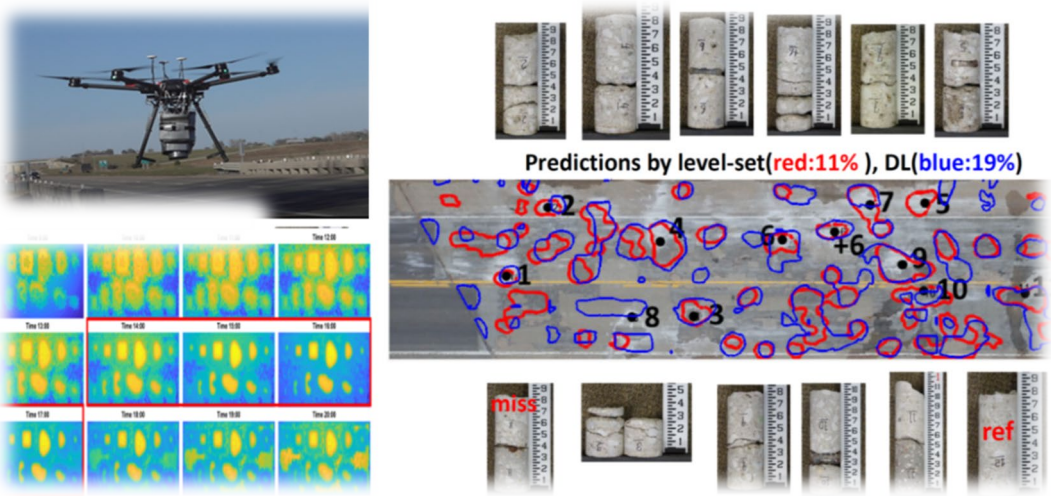

Sponsored By

Nebraska Department of Transportation and U.S. Department of Transportation Federal Highway Administration

December 31st, 2020

NEBRASKA
Good Life. Great Journey.
DEPARTMENT OF TRANSPORTATION

University of Nebraska Lincoln

University of Delaware 1743

TECHNICAL REPORT DOCUMENTATION PAGE

1. Report No. SPRP1(20) M109	2. Government Accession No.	3. Recipient's Catalog No.
4. Title and Subtitle To Automate Detecting, Quantifying and Mapping of Delamination via Arial Thermography		**5. Report Date** December 2020 **6. Performing Organization Code**
7. Author(s) Zhigang Shen[1], Chongsheng Cheng[1], Ri Na[2], Zhexiong Shang[1]		**8. Performing Organization Report No.** If applicable, enter any/all unique numbers assigned to the performing organization.
9. Performing Organization Name and Address [1] Durham School of Architectural Engineering and Construction 113 Nebraska Hall, University of Nebraska – Lincoln [2] Department of Civil and Environmental Engineering 342B DuPont Hall, University of Delaware		**10. Work Unit No.** **11. Contract** SPRP1(20) M109
12. Sponsoring Agency Name and Address Nebraska Department of Transportation Research Section 1400 Hwy 2 Lincoln, NE 68502		**13. Type of Report and Period Covered** Final Report July 2019 to December 2020 **14. Sponsoring Agency Code**

15. Supplementary Notes
If applicable, enter information not included elsewhere, such as translation of (or by), report supersedes, old edition number, alternate title (e.g. project name), or hypertext links to documents or related information.

16. Abstract
The goal of this project is to develop a UAV-based Arial thermographic method to detect and map the delamination on concrete bridge decks. Several image processing methods such as level-set and machine-learning were developed in this project. The developed method is high-efficient and low-cost and requires no-traffic-closure during the surveying process. The coring outcomes from four different concrete bride decks validated the performance of this developed method. The coring results suggested that this method outperformed several existing methods in detecting delamination in concrete bridge decks in terms of efficiency, accuracy, cost, and safety.

17. Key Words	18. Distribution Statement
drones, infrared imagery, concrete delamination, bridge deck, time windows, coring validation, automatic segmentation, level-set, machine learning, image processing	No restrictions. This document is available through the National Technical Information Service. 5285 Port Royal Road Springfield, VA 22161

19. Security Classification (of this report)	20. Security Classification (of this page)	21. No. of Pages	22. Price
Unclassified	Unclassified	Enter the total number of pages in the report, including front cover and appendices.	

Form DOT F 1700.7 (8-72) Reproduction of completed page authorized.

DISCLAIMER

The contents of this report reflect the views of the authors, who are responsible for the facts and the accuracy of the information presented herein. The contents do not necessarily reflect the official views or policies neither of the Nebraska Department of Transportations, nor the University of Nebraska-Lincoln and the University of Delaware. This report does not constitute a standard, specification, or regulation. Trade or manufacturers' names, which may appear in this report, are cited only because they are considered essential to the objectives of the report.

The United States (U.S.) government and the State of Nebraska do not endorse products or manufacturers. This material is based upon work supported by the Federal Highway Administration under SPR-P1(M109). Any opinions, findings and conclusions or recommendations expressed in this publication are those of the author(s) and do not necessarily reflect the views of the Federal Highway Administration.

ACKNOWLEDGEMENTS

The research team would like to thank Nebraska DOT for their tremendous field assistance during the coring validation phase. The research team would also like to thank the TAC members for their logistic assistance and technical feedbacks that helped to keep the project right on track. Without their hard work during the Covid-19 pandemic and under the scorching summer sun it would be impossible for us to have achieved the project goal without delay. The research team was especially impressed by and benefited from Mr. Jeremy Weigel's rich knowledge about deck coring, and his amazing maneuvering skill to back the big coring machine to the precise locations of the requested core samples.

Last, not least, the research team would like thank Mr. Guanyao Xu for his assistance in field data acquisition trips.

List of Figures

List of Tables

Table of Contents

1. Introduction

Concrete bridge decks are the most widely used bridge decks in the world due to their apparent advantages in operation performance, durability, cost, maintenance, and construction. Deck delamination is a major issue that negatively affects the longevity and serviceability of concrete bridge decks. The ratio of the delamination areas over the whole deck area is an important factor for decision making of deck repair and replacement. Since delamination mostly occurs in the subsurface of the deck and is invisible to the naked eyes, many non-destructive evaluation (NDE) technologies have been developed to detect and locate these delamination. Despite decades of effort and investment in developing these detecting and locating technologies significant issues still exist, which prevent DOTs from conducting quick, accurate, affordable, and safe bridge deck evaluations. In this report, the authors introduce a significantly improved infrared thermographic (IRT) technology based on the team's developed drone platform and image-processing methods. The research outcomes suggested that this newly developed IRT technology outperformed many existing delamination NDE technologies in terms of its efficiency, accuracy, cost, and safety when applied in the field environment.

In this report, the background, scope of work, project methodology, and results from the 33 bridge decks are described. The report is concluded with best practices and recommendations for using the developed technology.

1.1. Background

Timely detecting delamination/debonding issues of concrete bridge decks is essential to the safety of transportation and to make informed maintenance decisions. Many NDE methods (such as GPR, impact echo, chain dragging, half-cell, acoustic, and thermography) have been developed to identify these subsurface defects. Each of the developed methods has its pros and cons in terms of cost, safety, accuracy, reliability, and operability. Most of these methods need to have traffic closures when conducting the detections, which often cause substantial traffic delays and safety concerns for bridge users and DOTs. Therefore, delamination /debonding detection cannot be performed as often as necessary to have the most updated deck data for optimal decision making.

IRT methods are based on heat transfer physics as shown in Figure 1. The principle of applying the thermography for subsurface anomaly detection is based on the temperature difference between solid and debonded areas. The near surface delamination or void (depths ranging from ½" to 6") is treated as a thin air layer that blocks the directional heat transfer between the top and bottom of a reinforced concrete slab. Consequently, the average heat transfer rates are different between the delam areas and sound areas along the vertical direction. As a result, the surface temperature of the debonded area is higher than the solid area under the influence of solar radiation energy (Figure 1).

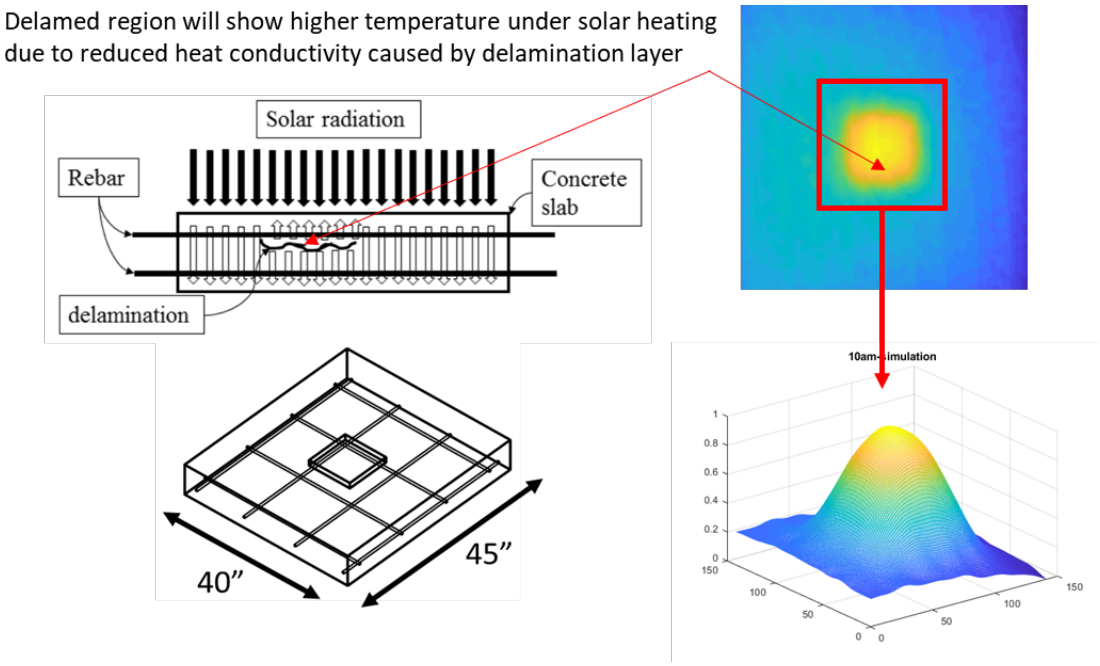

Figure 1. An illustration of basic heat transfer physics in the concrete delamination region

Despite the simple heat transfer theory, many environmental noises such as surface debris, strong textures (deep scratches, grooves, cracks etc.), dark color coating etc., could create complex temperature background noises. In field practices, mixed results were reported by state DOTs using earlier IRT detection methods, which relied on hand-held or vehicle-mounted thermal cameras for data collection of deck surface temperatures [1 to 5]. For example, Iowa DOT did a series of studies from 1982 to 2013 on using thermal images to detect pavement/deck delamination [1, 3, ,4].

Notably, almost all these projects used raw thermal images to detect delamination. None of them used any noise deduction image processing technologies or filters. Major challenges facing these earlier IRT methods include high background noise, low-resolution, distorted thermal images, and the lack of proper image processing capability to segment the delam areas. Subsequently, the outcomes of these methods were highly susceptible to the environmental noises such as surface textures (such as grooving, tining, cracks, small foreign gravels etc.). These challenges hindered the further adoption of the thermographic method as a viable detecting approach.

Recent technical advancements in image processing and UAV technology have the potential to transform the IRT-based approach to detect delamination/debonding in concrete decks. The three most relevant new technical advancements are:

1) new algorithms in computer vision to detect edges and recognizing objects in high noise situation.

2) new image processing techniques for distortion correction and image stitching for creating seamless and accurate full deck images; and

3) high-resolution thermal and optical cameras mounted on drones to take close-up aerial thermal and optical images of the bridge decks to capture the smallest temperature resolutions of the deck surfaces. As a result, the revitalization of research activities in thermographic detecting was recently witnessed with improved outcomes [6-9].

Existing studies made efforts on handling the thermal image from multiple aspects of temperature histogram in the threshold method [6], temperature density in the k-mean clustering method [7], and temperature spatial relationship in region growth method [8,9]. So far, these reported methods to distinguish the delaminated area from the sound area were primarily based on evaluating the temperature contrast at the global level of the inspected decks, which often led to either over-estimate, or to under-estimate the quantities of the delaminated areas.

1.2. Objectives

The primary goal of this project is to validate the effectiveness of the developed new IRT technology, which is based on a drone-based data acquisition platform and the developed image processing methods. The validation will be through lab experiments and field coring samples. The performance of the developed technology is measured in two aspects: accuracy and efficiency in detecting, quantifying, and mapping delamination of bridge decks.

There are four specific objectives in this project:

1) To validate the proposed Aerial IRT approach in detecting, quantifying, and mapping delamination in bridge decks. The plan is to collect thermographic and optical image data of 33 candidate bridges identified by NDOT, and to predict the delamination maps of the decks through the developed image processing technology. The targets are concrete bridge decks, including low-slump decks and monolithic decks.

2) To identify the best timing and weather conditions for thermographic surveying through numerical simulations. Numerical simulations will be conducted to identify the best timings to conduct thermographic bridge deck survey across seasons in Nebraska by using boundary condition data from local weather stations. The results of the numerical simulations will be validated by outdoor lab experiments on the University of Nebraska - Lincoln campus.

3) To develop automated detection, quantification, and mapping methods of concrete deck delamination.

4) To develop a best practice guidelines and recommendations for the application of Arial IRT technology using the experience gained from the project.

1.3. Expected Benefits

Compared to other existing NDE methods, the developed drone based IRT technology has notable benefits:

a. Safe, low-cost, and easy to deploy. Since the introduced technology does not affect the normal traffic flow during the inspecting process the potential accidents due to interrupted traffic flows and lane closures are minimized. The extra costs of lane closures and traffic maintenance required by other methods (such as chain dragging, hammer sounding, impact echo, and other acoustic methods), are therefore saved. The logistic needs for this approach are minimal. A two/ three-person crew and all the equipment in a SUV can be deployed to one or multiple inspection sites with little preparation time.

b. Highly efficient. The typical flying speed of the drone in this proposed project is roughly 4 mph in the air 120 feet or higher above the deck during operation, which can cover 4-lane width (approx. 50 ft) with one single high-resolution thermal image. Therefore, it took about 45 to 90 minutes (including times for initial on-ground calibration, set up and wrap-up) to conduct a full-coverage thermographic survey of a 6-lane (2 lanes on each bound plus shoulders) 400-feet long bridge decks. Such level of efficiency is difficult to match by other NDE delamination detecting methods. Since there are more than two thousand of bridges in Nebraska alone, this high-efficient approach will allow closer and more frequent monitoring of the bridge deck conditions without worrying delaying traffics.

c. Accurate and precise. Since the images used in generating the delamination maps in the proposed method are orthophotos (Aerial-view) of the bridge decks, image distortion and stitching errors are minimal compared to delamination maps created by stitching many perspective-view images from the ground vehicles. The less-distorted aerial images of the bridge deck enable people to create highly accurate and precise delamination maps of the bridge decks. Many potential benefits can be achieved from the high accuracy delamination maps. One example is that it enables us to monitor the formation of the delaminated areas over time. Another benefit is that it makes the coring validation much easier because the location of the delamination can be determined with an accuracy of 2-3 inches.

d. Versatile. The drone-based thermography can be used to detect delamination of other bridge elements, such as the vertical or slanted concrete surfaces, which are difficult to access using other NDE methods. These vertical elements can be parapet walls, wing walls, girders, and abutment walls, etc.

1.4. Project Scope of Work/Tasks

In order to achieve the goal and objectives the following scope of work/tasks were developed in this project:

a. Data Acquisitions

Four sources of surface image data of concrete decks were collected and used in this project:

1) lab experimental data of the casted indoor and outdoor concrete slabs with artificial delamination.

2) surface temperature distribution data from numerically simulated concrete slab cases

3) field image data of in-service concrete bridge decks

4) coring sample data of concrete bridge decks

a.1) Lab experimental data used in this research was acquired in August and September of 2018 from four casted concrete slabs with artificial delamination at three different depths. High resolution (4K) RGB images and mid-wave (3-5 μm) infrared thermographic (IRT) images of the top surface of these slabs were taken. 8 to12 hours IRT data of the four casted slabs was recorded continuously during the day by a FLIR A8300sc camera as shown in Figure 2.

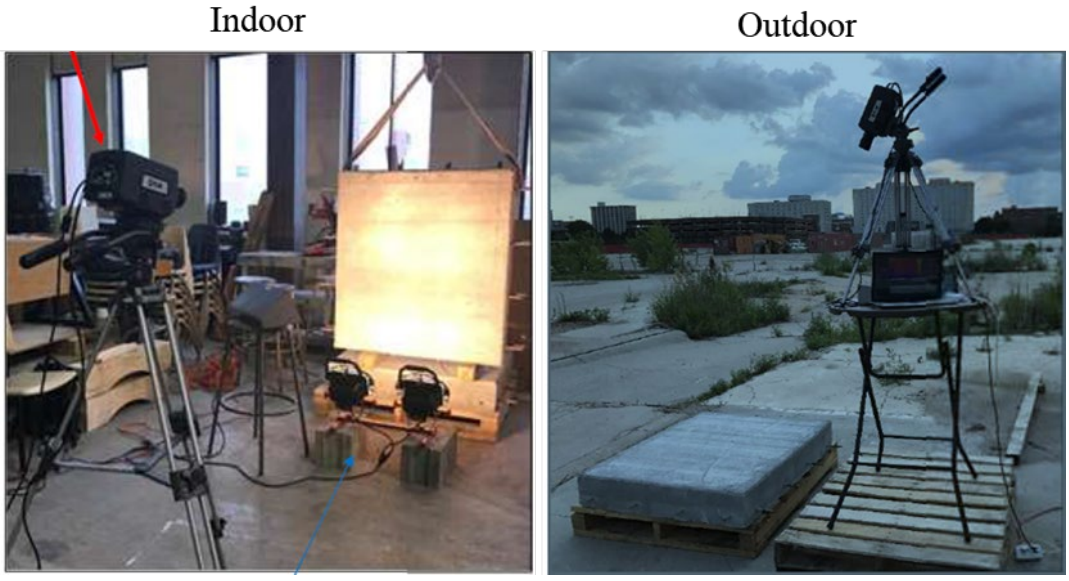

Figure 2. Experimental data acquisition settings

a.2) Numerically simulated surface temperature data of concrete decks provided many insights in explaining the physical surface temperature distribution of concrete slabs under solar radiation. These insights are hard to get or expensive to get by physical lab experiments since casting several 7 ½" thick 15'x30' concrete slabs at different geographical locations will cost a lot if possible. However, in numerical simulations any sizes of slabs can be created at any geographical locations without incurring significant extra costs. By simulating daily surface temperature variations of delaminated concrete decks in different seasons the best time windows for IRT surveying were identified. Examples of the numerical simulations of the transient heat transfer process are illustrated in Figure 3.

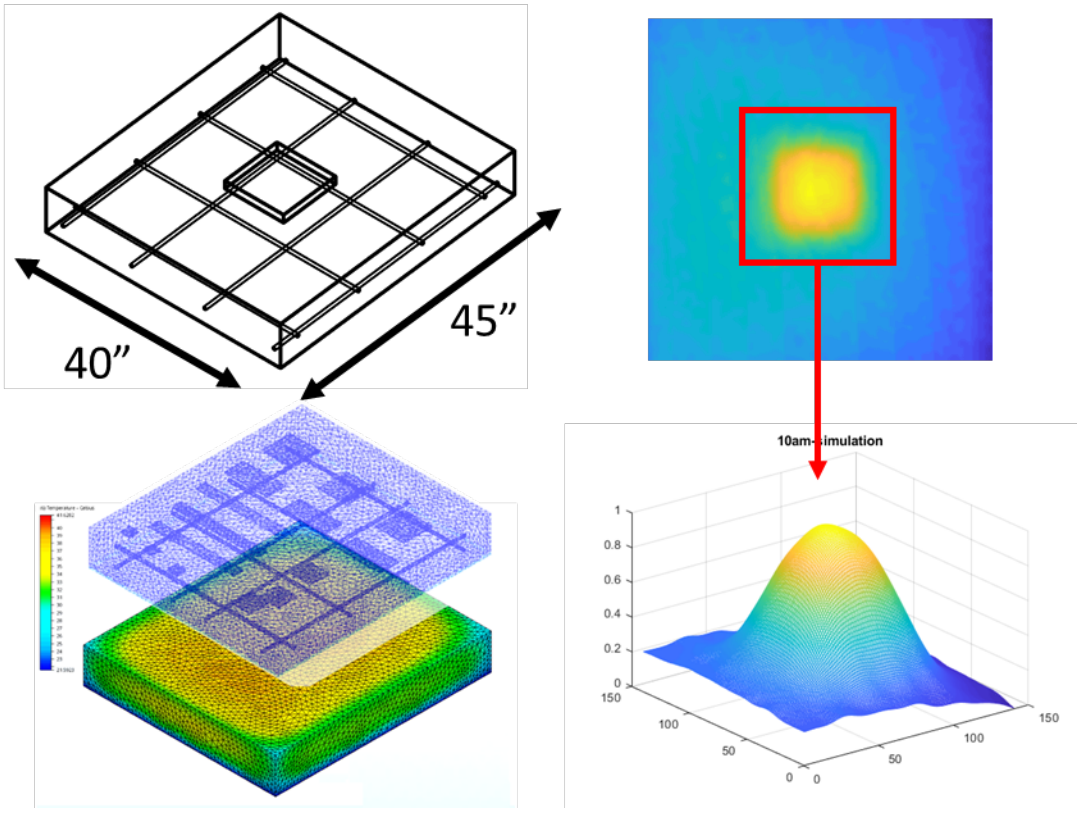

Figure 3. Examples of the numerical simulation of the transient heat transfer process with delamination in the concrete decks

a.3) Field data of high resolution (4K) RGB images and mid-wave (3-5 μm) IRT images of the thirty-three (33) in-service bridge decks (See Table 1) were acquired using the drone platform (Figure 4) during September and October in 2019. All these deck images were taken between 1:00 PM and 5:00 PM since the quality of IRT images are

timing-sensitive, and this time window is deemed the best in September and October from our numerical simulation results.

Figure 4. Equipment used for field data acquisition of bridge decks (Left to right: FLIR A8300 camera, DJI M600 drone, DJI X5 camera, and DJI Inspire 1 drone)

Table 1. The surveyed thirty-three bridge decks and their wearing surface types.

No.	BRIDGE_ID	Wearing surface
1	S030 42623L	1 Monolithic Concrete
2	S043 02621	1 Monolithic Concrete
3	S045 00552	1 Monolithic Concrete
4	S056 02857	1 Monolithic Concrete
5	S057 05832	1 Monolithic Concrete
6	S057 06092	1 Monolithic Concrete
7	S057 06312	1 Monolithic Concrete
8	S057 06460	1 Monolithic Concrete
9	S057 06507	1 Monolithic Concrete
10	S057 06733	1 Monolithic Concrete
11	S069 07226	1 Monolithic Concrete
12	S080 37312	1 Monolithic Concrete
13	S080 39165L	1 Monolithic Concrete
14	S080 39165R	1 Monolithic Concrete
15	S080 39294L	1 Monolithic Concrete
16	S080 39294R	1 Monolithic Concrete
17	S080 40375R	1 Monolithic Concrete
18	S103 00417	1 Monolithic Concrete
19	S129 00150L	1 Monolithic Concrete
20	S008 02034	2 Integral Concrete
21	S080 36314L	2 Integral Concrete
22	S080 36314R	2 Integral Concrete
23	S080 36153L	4 Low Slump Concrete
24	S080 36153R	4 Low Slump Concrete
25	S080 37731L	4 Low Slump Concrete
26	S080 37731R	4 Low Slump Concrete
27	S129 00038	4 Low Slump Concrete
28	S129 00150R	4 Low Slump Concrete

29	S015 08239	6 Bituminous
30	S036 02040L	6 Bituminous
31	S041 08450	6 Bituminous
32	S092 46256R	Unknown (missing data from NDOT)
33	S092 46282R	Unknown (missing data from NDOT)

It took 10 daytrips to acquire the field data of the thirty-three (33) bridge decks (see Figure 5 for the locations of the surveyed bridges decks and the dates of the aerial surveys). Depending on the geospatial locations of the bridges, weather conditions, and the size of the bridges, the number of bridge decks were surveyed in one day ranged from two to seven bridge decks. The average survey time for a three to four-lane bridge deck is between 45 minutes to 90 minutes including setup and wrap-up time, which out-performed most existing delamination segmentation technology in terms of efficiency.

For decks that are close to each other the average survey time can be much shorter. For example, surveying both S080 36153L and S080 36153R bridge decks (three lanes each including shoulder) only took a few minutes longer than surveying a single 3 or 4 lanes bridge deck since the two can be surveyed together with only one setup and one wrap-up time. Taking the GPR array as an example, a GPR array mounted vehicle may survey a deck at a driving speed of 60 mph. However, this type of detection equipment can only scan one lane on each pass. For this type of GPR vehicles to exceed the performance of drone IRT method it will need six this kind of GPR vehicles to run altogether in two opposite bounds to scan the 6 lanes in the S080 36153 L&R deck case. In the future, if the decks are changed to 4 lanes the drones survey time will remain pretty much the same and the GPR array method will need eight vehicles to exceed the drone survey speed. The drone has a clear advantage in terms of efficiency.

Vehicle mounted IRT method will have the similar efficiency to the vehicle mounted GPR array since it can only scan one lane at each pass. Plus, for a IRT camera to work at a vehicle speed of 60 mph the camera needs to have a high framerate (60fps or above) at a full resolution (1080p), which exceeds the capacity of most IRT cameras on the market cost $100k or less.

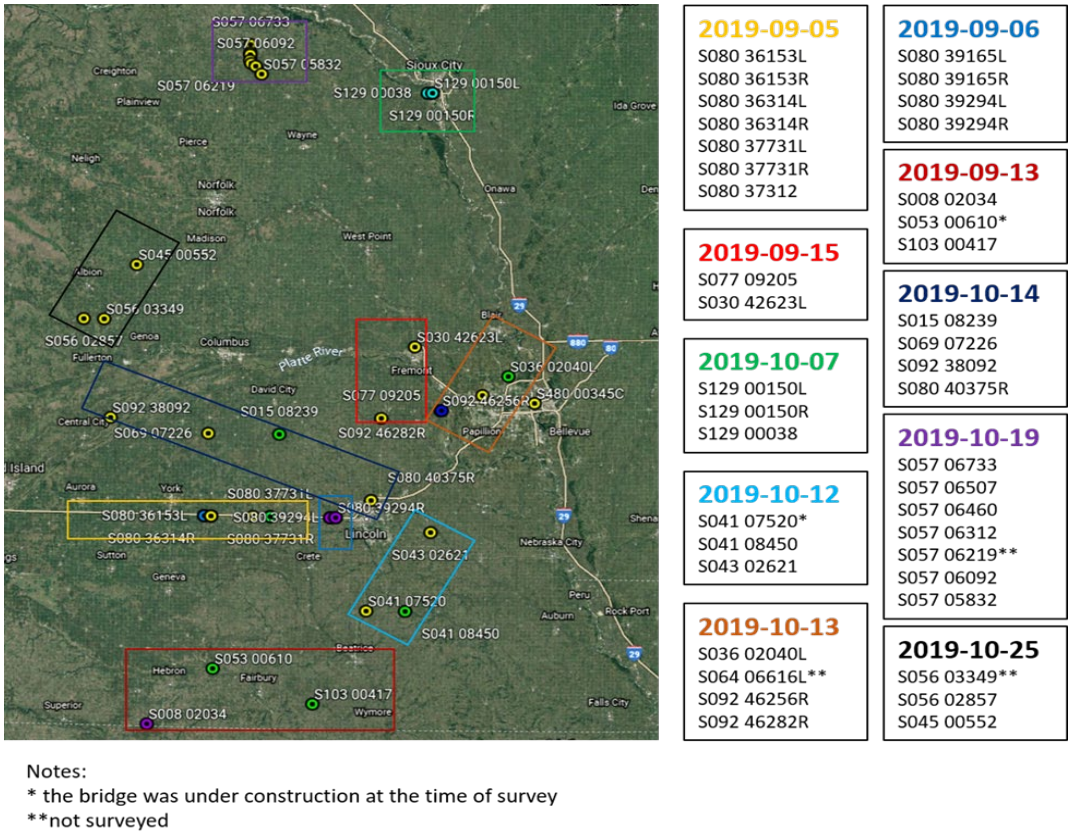

Figure 5. Locations of the surveyed bridge decks and the dates of the Aerial surveys

a.4) Validation data were collected from coring samples of four bridge decks, two of which have low slump covering and the other two decks are monolithic (Table 2). The coring activities started in and lasted through the summer of 2020. The decision of selecting the four bridge decks for validation was based on NDOT's construction schedule and the team's survey outcomes where the decks were predicted having significant amount of delamination. Table 2 shows the four bridge decks chosen for coring validation. Figure 6 shows one example of the coring data, where the core sample locations (black dots) in related to the predicted delamination areas (red and blue shapes on the deck) are illustrated.

Table 2. Four (4) selected bridge decks for collecting coring validation data

Bridge ID	Deck type	Coring date(s)	Coring
S080_37312	Monolithic	06-03-2020, 07-23-2020	20
S103_00417	Monolithic	06-04-2020	14
S080_37731L	Low slump	06-03-2020	12
S080_36153L	Low slump	07-14-2020	13

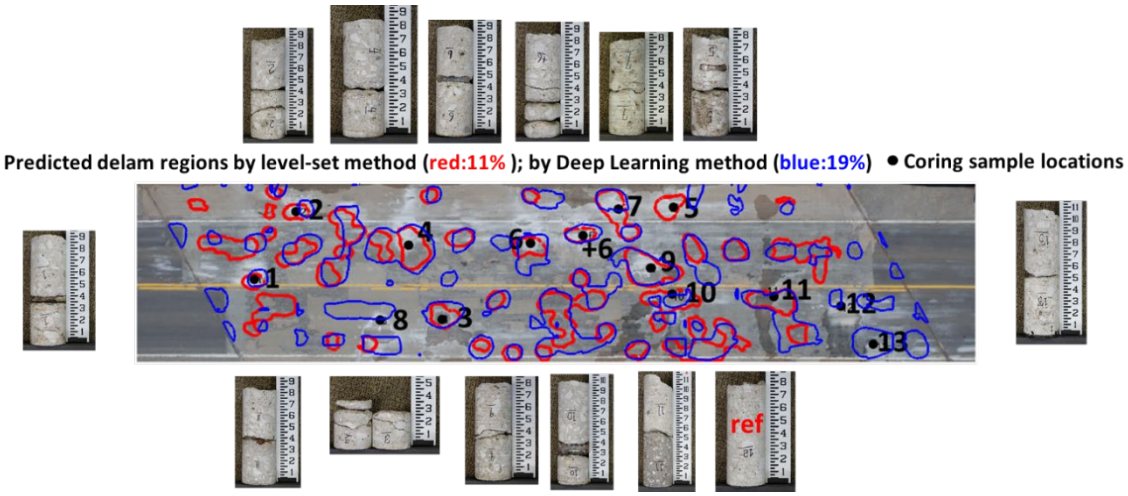

Figure 6. An example of the collected coring data from S103_00417 bridge deck

b. Development of Image Processing Methods

The key for the success of the project is to develop new image processing and segmentation methods that can handle the high noise and uneven background from the IRT images due to the rough surface textures and frequent foreign debris on the concrete bridge decks. Three different image processing and segmentation methods were developed and validated: 1) the grayscale morphological reconstruction method [13]; 2) the gray-scale level-set method [14]; and 3) the machine learning method [15]. Among the three methods, level set method demonstrated the most robust performance. And the three methods can be used together to increase the performance of the delamination segmentation and to increase the confidence level with the predicted results.

The technical and implementation details of the three image segmentation methods can be found in the corresponding journal publications [13,14,15].

c. Identification of the Best Time Windows for Aerial IRT

Field IRT detection of concrete delamination relies on temperature contrast and temperature gradience caused by solar heating. It takes time for concrete bridge deck to warm up by the solar radiation to reveal the delaminated deck regions. The bridge deck heating process is also influenced by the seasonal environmental factor such as the intensity of solar radiation, ambient temperature, diurnal temperature fluctuation range etc. Therefore, there exists optimal IRT detection windows during the day, when the temperature contrast and boundary gradience reach the highest between the delaminated regions and the non-delaminated regions. However, there were few systematic studies to provide convincing evidence to identify the optimal time windows for IRT detection.

As part of the scope of work of this project, the research team conducted a series of lab experiments and numerical simulations to identify the best time windows to provide guidance for future field implementation of IRT detection of delamination. And the outcome of these studies provided convincing evidence to support our conclusion about the optimal time windows.

d. Validation

In this project coring samples were used to evaluate the accuracy of the predictions by the developed image processing methods. Coring outcomes were also used to further calibrate the prediction model, and to increase the accuracy and robustness of the prediction model. Since the location accuracy of the developed segmentation methods can reach within inches, which is comparable to the accuracy of hammer sounding method, coring or hammer sounding can provide a good validation for the prediction models. The accuracy or spatial resolution of many other NDE methods were measured by foot or feet, and therefore, to apply coring validation will be difficult since the delam locations cannot be located accurately like hammer sounding method. For example, the accuracy of impact echo method relies on the grid sizes, which determines its maximum accuracy. The accuracy of the vehicle mounted GPR (Ground Penetrating Radars) array method will eventually rely on the density and layout of the array, but it is difficult for GPR array to achieve location accuracy of inches using the current GPR technology even with a RTK aid.

Fifty-nine (59) coring samples from four bridge decks were taken (Table 2) at the locations that were field measured by distance measuring wheel and Bosch Blaze 400 feet laser Measure. The diameters of the coring samples were 3 inches or 4 inches. The coring depths of the samples ranged from 6 inches to 8 inches. Figure 7 shows one example of field marking of coring sample locations and the field measure tools.

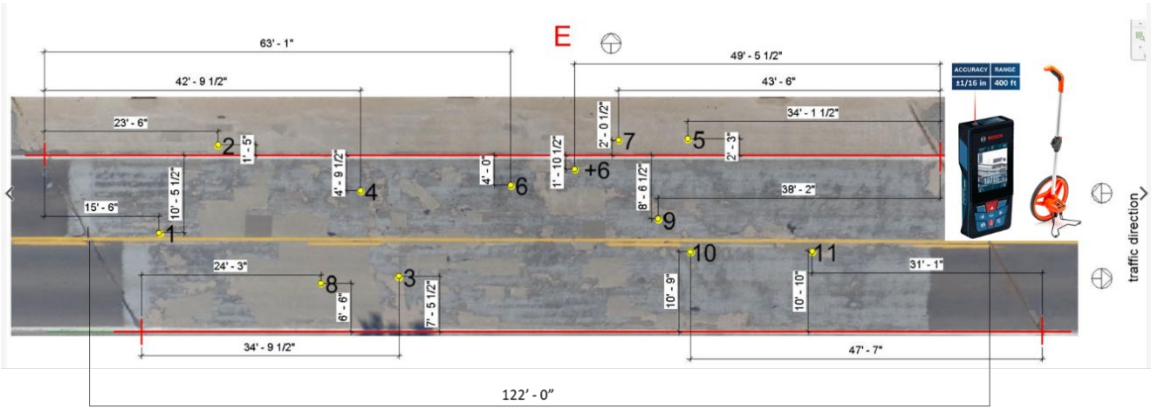

Figure 7. An example of marking coring sample locations on Bridge S103_00417

e. Best Practice and Recommendations

To facilitate the implementation of the developed Aerial IRT technology in Nebraska DOT, a summary of the best practices and recommendation is included in this report. This summary is based on the team's filed experience of surveying the 33-bridge decks, and other bridge decks over the past three years. The summary includes recommendations of cameras and drone choice, field survey planning, field survey operation, data acquisition, survey crew, safety considerations, weather conditions, survey time windows, data flow, and post-processing of image data.

2. Research Methodology

Figure 8 illustrates the research methodology to carry out the project. There are four major research tools employed in this study to support the development of the image segmentation methods, and performance evaluations of the methods: 1) lab experiments; 2) numerical simulations; 3) image processing algorithms, and 4) field coring validation. The four tools were employed in the three consecutive steps.

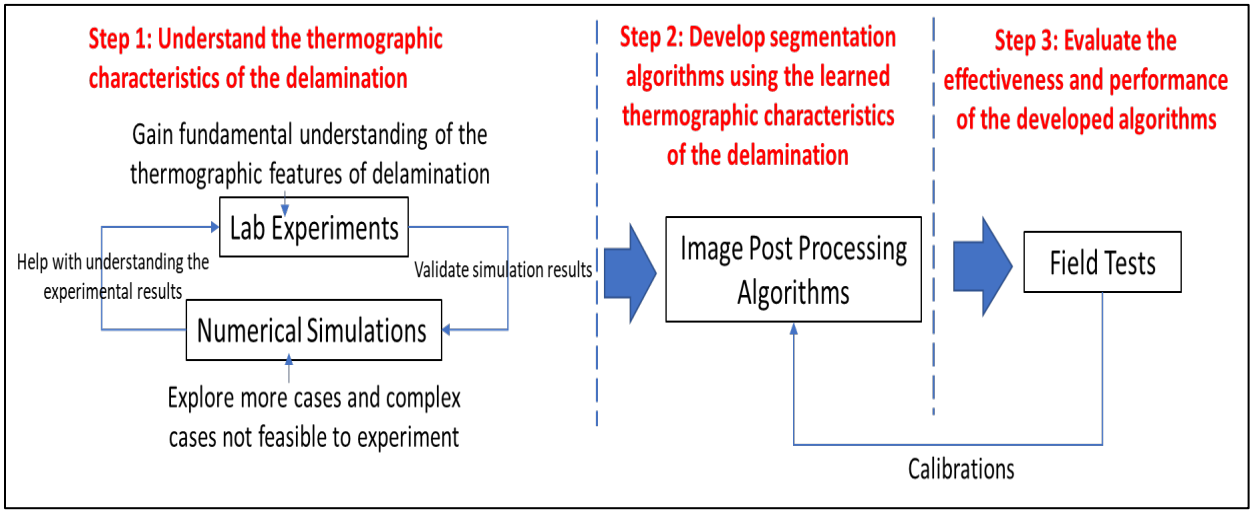

Figure 8. Schematics of the research methodology

2.1 Lab Experiments

An experimental study was conducted using artificial delamination in the three 4'x4' reinforced concrete slabs on the University of Nebraska-Lincoln campus. The outdoors location had full sun all day long. The reinforced concrete slabs are illustrated in Fig. 9. A Styrofoam board of size 1'x1' was embedded at the center of each slabs at the depths of 2", 3", and 4" respectively from the top surface of the slab. The thickness of foam is about ¼" with the thermal conductivity about the same as a thin layer of air. The slabs were casted and cured indoors over 28 days and then moved outside for data collection. A FLIR A8300sc thermal camera was used to collect the surface temperature data and to capture thermal images for further processing to segment

delamination regions. Figure 10 shows a snapshot example of the recorded thermal images and delamination characteristics of the three experimental slabs.

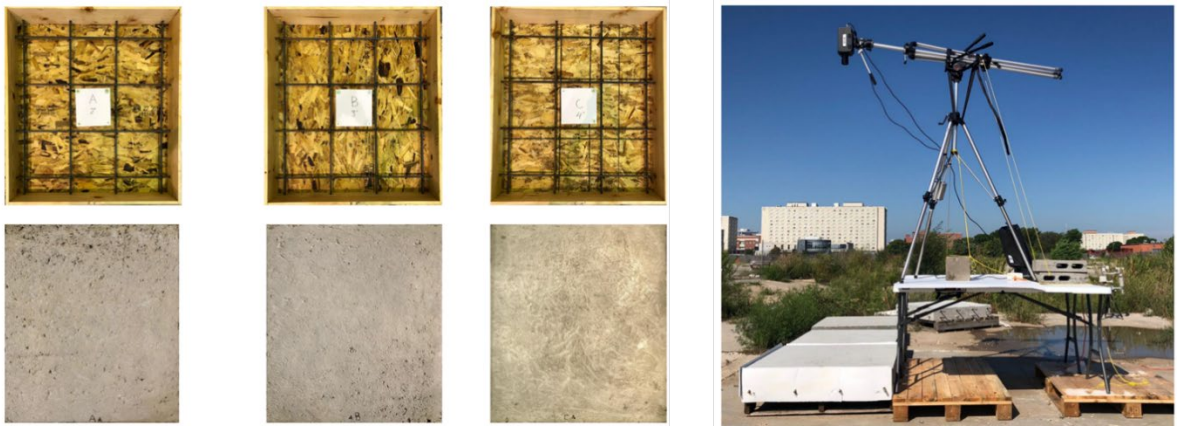

Figure 9. Experimental Specimens and IRT image recording settings.

Fig.10 illustrates several variations observed by constructed samples under the natural thermal cycle of the day. It shows the thermal images of three mimicked delamination buried at different depths in the concrete slabs at different time windows. The red dash box shows the true size of the delamination. Fig.10a shows the thermal image of the delamination at 11 am with depth of 4.5 cm (left), 7 cm (middle), and 9.5 cm (right) from the top surface. The shallower delamination has more temperature contrast than the deeper one at the same time window. Fig.10b shows the temperature profile of the section (black dash line) at a different time of the day. It reveals that the average temperature shifts at different time windows for the same slab. Fig.10c shows the preprocessed image by standardization (Eq.1), which is useful to remove the effect of temperature shifts.

$$I_s = \frac{I - m_I}{\delta_I}, \qquad (Eq.\ 1)$$

Where I refers to the raw thermal image, m_I is the mean temperature of I, δ_I is the standard deviation of I. The standardized image I_s represents the temperature deviation from its own mean at the current time. Through the Fig.1c, the contrast variation between different depths and time windows are more clearly represented. To identify the best observation windows the recording was performed continuously throughout the day.

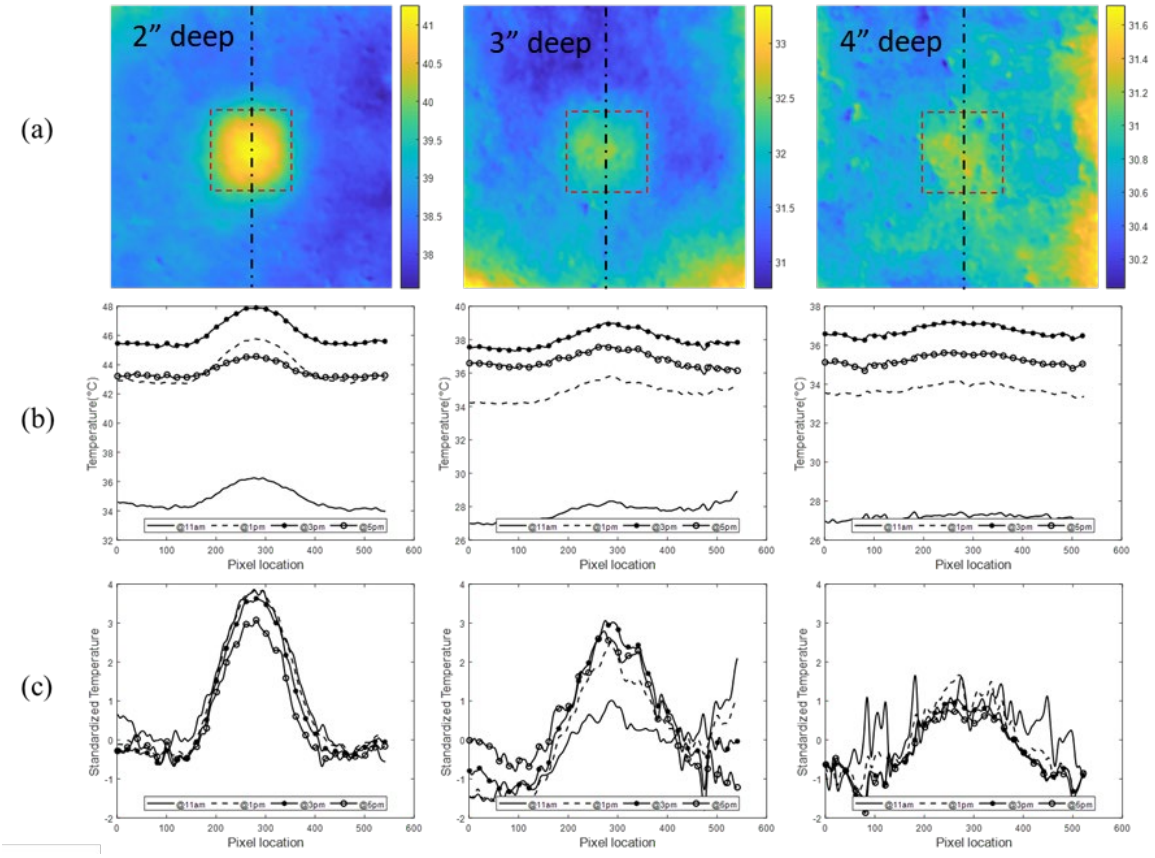

Figure 10. Examples of thermographic characterization of the delamination regions: (a) raw thermographic images; (b) raw temperature section profile along the vertical dash-dot center line; (c) normalized temperature section profile along the center line [15]

2.2 Numerical Simulations of Heat Transfer of Concrete Delamination

In the first step, heat transfer results from the numerical Computational Fluid Dynamics (CFD) simulations of the same slabs as the experimental ones were compared to the recorded experimental data (Figure 11). The effectiveness of the numerical simulations was validated.

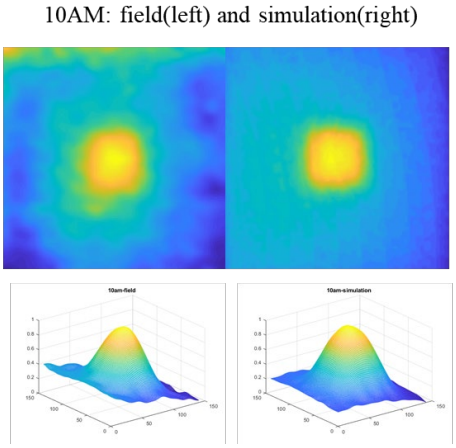

Figure 11. Validation of the numerical simulation results

Then a large slab that is closer to the actual size of concrete bridge decks was simulated to identify the best time windows for IRT surveys. The simulated slabs contained more complex delamination regions (Figure 12) so as to imitate the real bridge deck conditions, thus can provide more reliable outcomes.

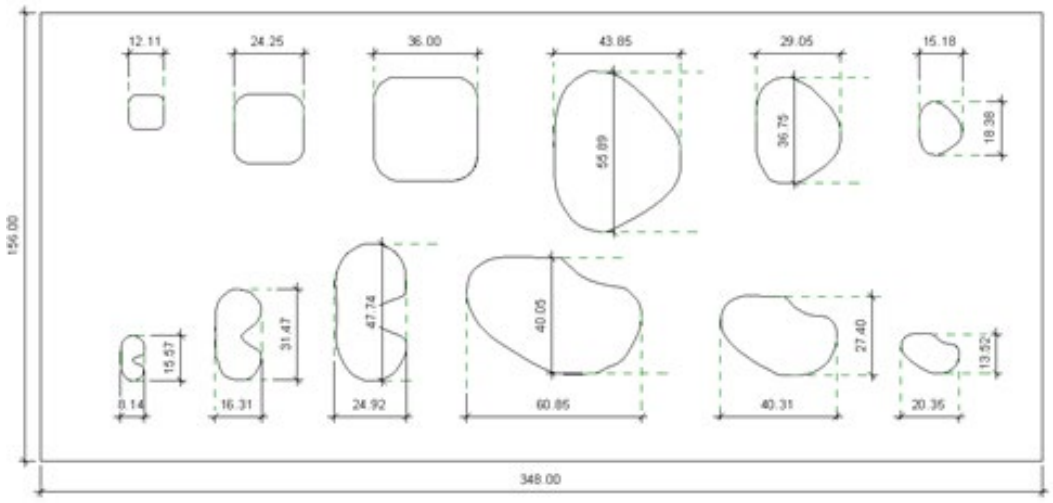

Figure 12. A more complex numerical slab of similar size to a real bridge deck (unit: inch)

2.3 Image Post Processing Methods

Three image processing algorithms were developed to capture the thermographic features of the delaminated regions, and then segment the region along the edges of the delamination.

a. Grayscale morphological reconstruction method [13]

"The Environmental and surface texture-induced temperature variation across the bridge deck is a major source of errors in delamination detection through thermography. This type of external noise poises a significant challenge for conventional quantitative methods such as global thresholding and k-means clustering. An iterative top-down approach is proposed for delamination segmentation based on grayscale morphological reconstruction. A weight-decay function was used to regularize the reconstruction for regional maxima extraction. The mean and coefficient of variation of temperature gradient estimated from delamination boundaries were used for discrimination." [13] Figure 13 is a graphical illustration of the basic idea of this method.

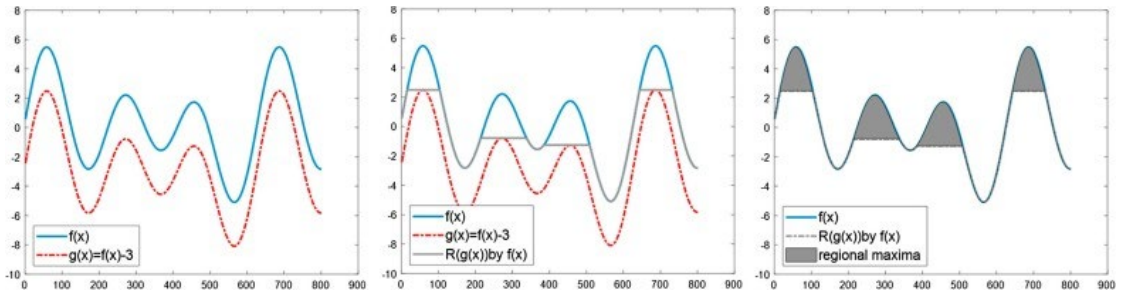

Figure 13. A graphical illustration of grayscale morphologic reconstruction for 1D representation: (a) synthetic 1 D signal f(x) = sin(x) + 2 * cos(2 * x + 5) + 3 * sin(3 * x) and g(x) = f(x)−3; (b) reconstruction of g(x) by f(x); (c) regional maxima by difference between f(x) and R(g(x)). [13]

b. Level-set segmentation method [14]

"Conventional nondestructive delamination detection of concrete pavements through thermography is often based on temperature contrasts between delaminated and sound areas. Non-uniform backgrounds caused by the environmental conditions are often challenging for contrast-based methods to robustly differentiate the delaminated areas from the sound areas. Instead of focusing on the temperature contrast, this study proposes a temperature gradient-based level set method (LSM) to detect boundaries for delamination segmentations. A modified edge indicator function is developed to represent the normalized temperature gradient of a thermal image." "The results demonstrated significant improvements compared to the well-accepted k-mean method in terms of accuracy and stability of the detections." [14].

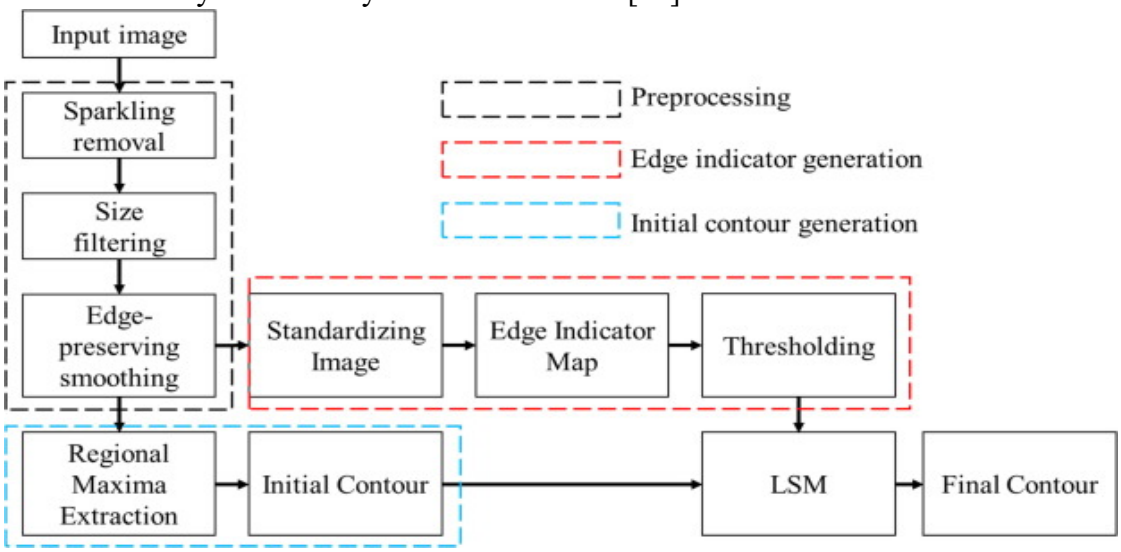

Figure 14. The diagram of the proposed level-set framework [14]

c. Deep Learning Method [15]

"Concrete deck delamination often demonstrates strong variations in size, shape, and temperature distribution under the influences of outdoor weather conditions. The strong variations create challenges for pure analytical solutions in infrared image segmentation of delaminated areas. The recently developed supervised deep learning approach demonstrated the potentials in achieving automatic segmentation of RGB images. However, its effectiveness in segmenting thermal images remains under-explored. The main challenge lies in the development of specific models and the generation of a large range of labeled infrared images for training. To address this challenge, a customized deep learning model based on encoder-decoder architecture is proposed to segment the delaminated areas in thermal images at the pixel level. Data augmentation strategies were implemented in creating the training data set to improve the performance of the proposed

model. The deep learning generated model was deployed in a real-world project to further evaluate the model's applicability and robustness. The results of these experimental studies supported the effectiveness of the deep learning model in segmenting concrete delamination areas from infrared images." [15]

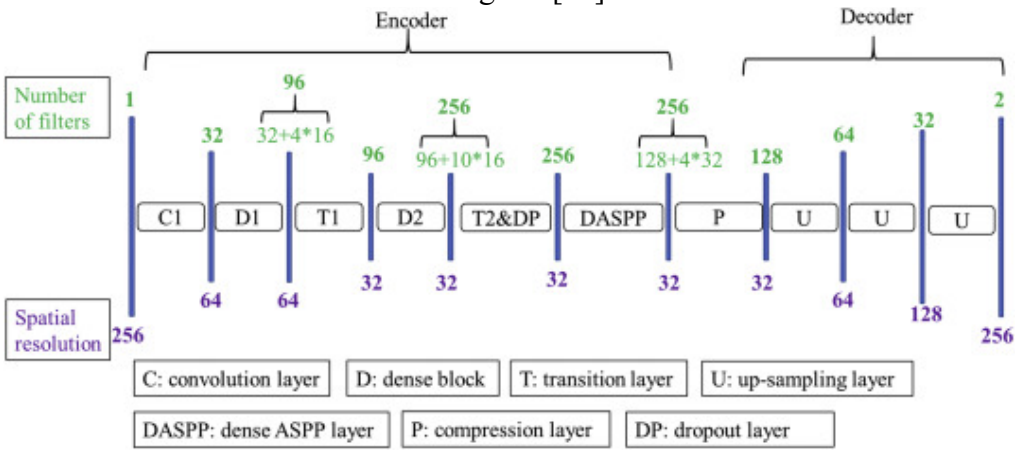

Figure15. The developed deep learning architecture [15]

2.4 Field Tests

Four in-service concrete bridge decks were selected for field tests to evaluate the effectiveness and performance of the developed technology in terms of its accuracy, robustness, and efficiency. Coring samples were used to assess the accuracy of predictions. The correct prediction rate (CPR) was used to measure it. The robustness performance was evaluated by the standard deviation of the CPRs (σ CPR) on the four bridge decks surveyed at different dates and times. The efficiency performance (EP) was measured by the estimated average work time spent on each bridge deck, which can be used to compare with other existing delamination survey methods.

$$CPR = \frac{the\ number\ of\ core\ samples\ with\ correct\ prediction}{total\ numerber\ of\ core\ samples}\ x\ 100\% \qquad \text{(Eq. 2)}$$

$$\sigma\ CPR = \sqrt{\frac{1}{4}\sum_{i=1}^{4}(CPR_i - \mu)^2} \qquad \text{(Eq. 3)}$$

3. Results

3.1. Delamination predictions of the twenty-nine bridge decks (excluding asphalt decks)

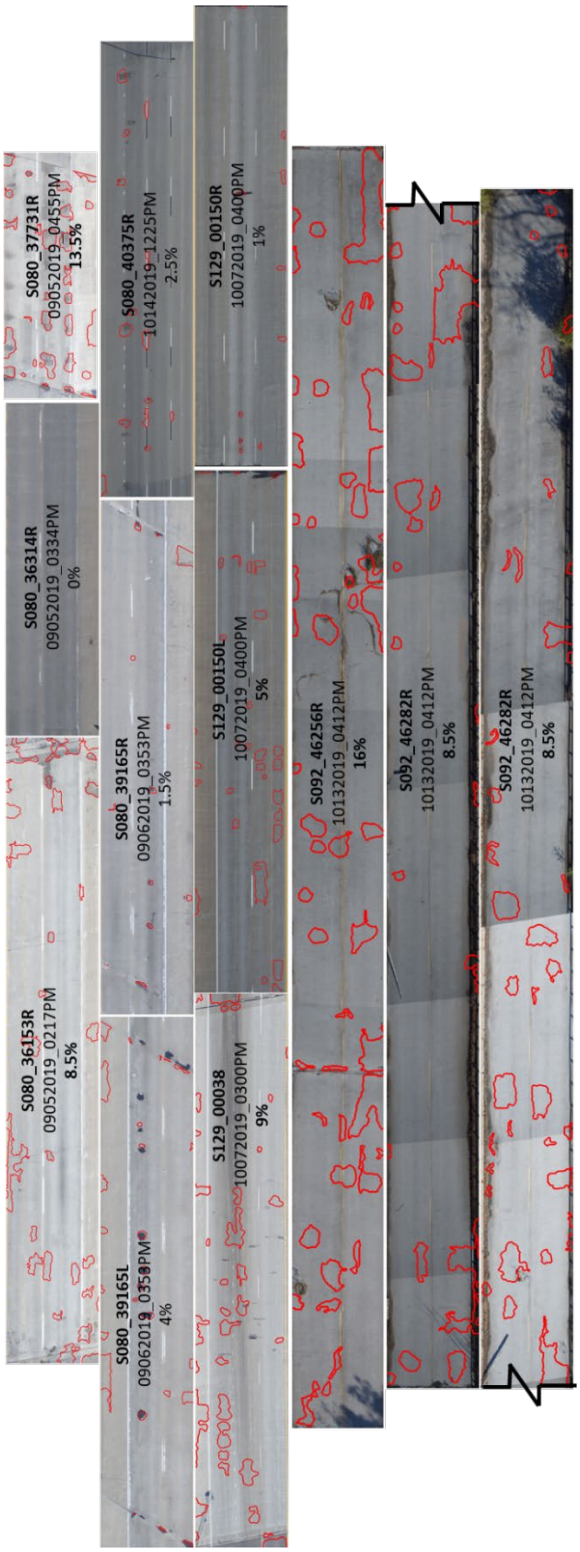

Figure 16. The delamination prediction results of the first 11 bridge decks

Note: The red shapes represent the predicted delamination regions. The percentage of the predicted delaminate is also labeled on each image

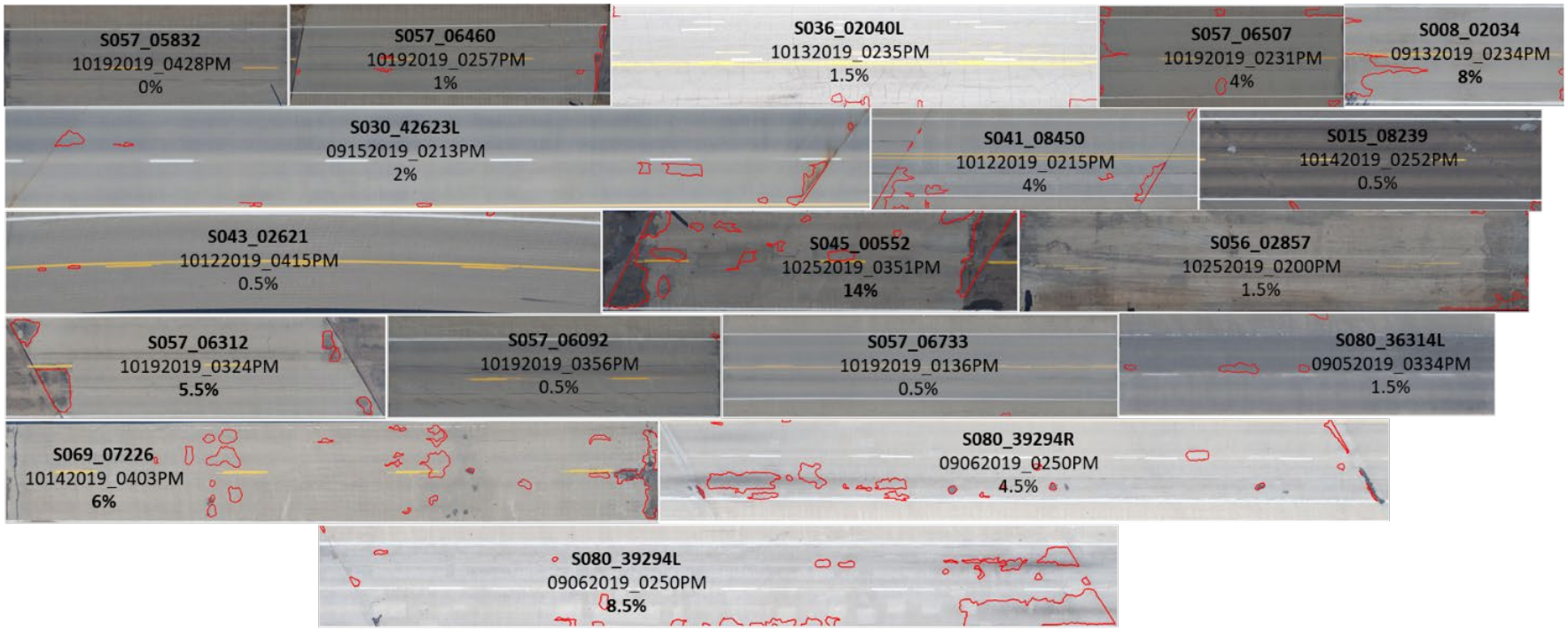

Figure 17. The delamination prediction results of the rest 18 bridge decks

Note: The red shapes represent the predicted delamination regions. The percentage of the predicted delaminate is also labeled on each image

3.2. Numerical Simulation Results

The results of the numerical simulations of a large size delaminated concrete deck were used to investigate the best time windows to conduct IRT surveys. After simulations of a total of six cases (3 delamination depths x 2 seasons) from 9:00 AM to 8:00 PM, the best time windows were identified as: 14:00 – 17:00 (2 PM –5 PM) in summer, and 14:00 – 16:00 (2 PM –4 PM) in fall. Please note this conclusion from the numerical simulations is not limited to the application in drone based IRT surveys. It can be applied in any IRT surveys including using other platforms such as vehicle-mounted or hand-held.

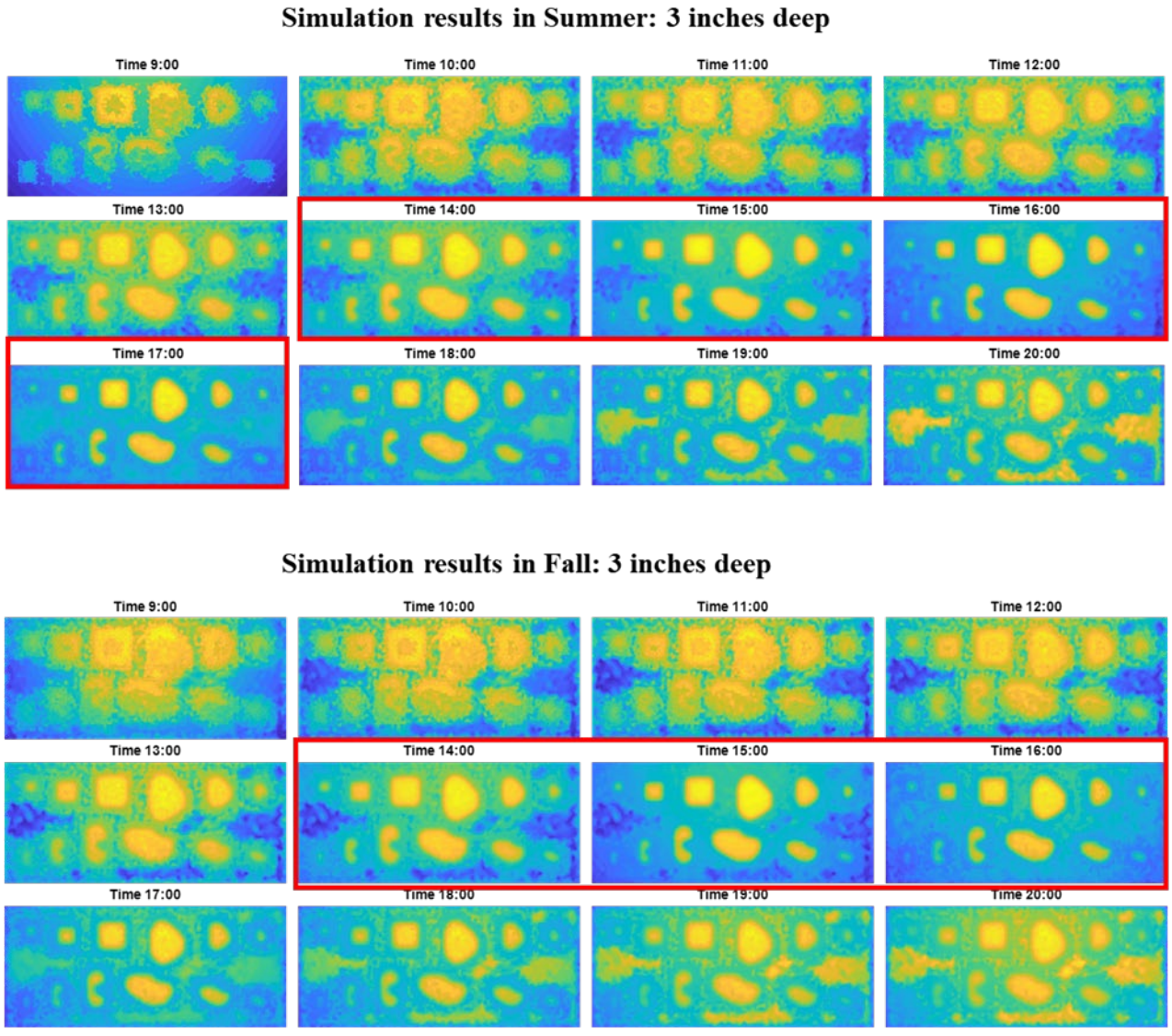

Figure18. A graphic example of the results of numerical simulations of the delaminated regions during the days in two seasons

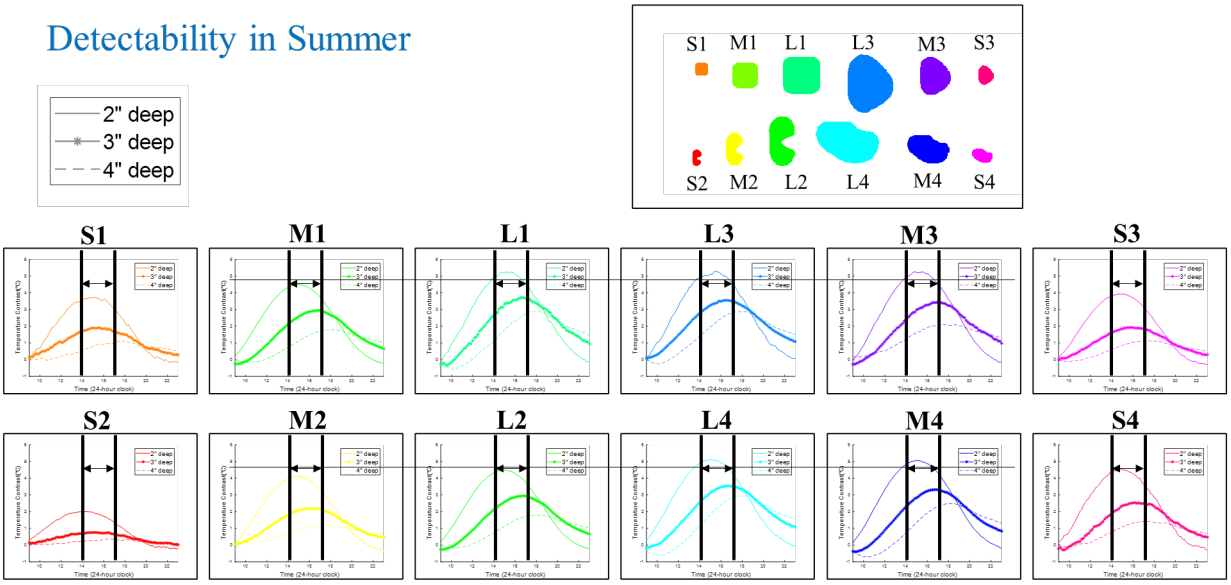

(1) During the optimal time window (**14:00 to 17:00**), the smallest (1 SF) and deepest (4 in) delam can develop a contrast of 0.5~1°C.
(2) the maximum contrast varies due to difference in size and depth (can be over 5°C for the largest delam at shallowest depth)

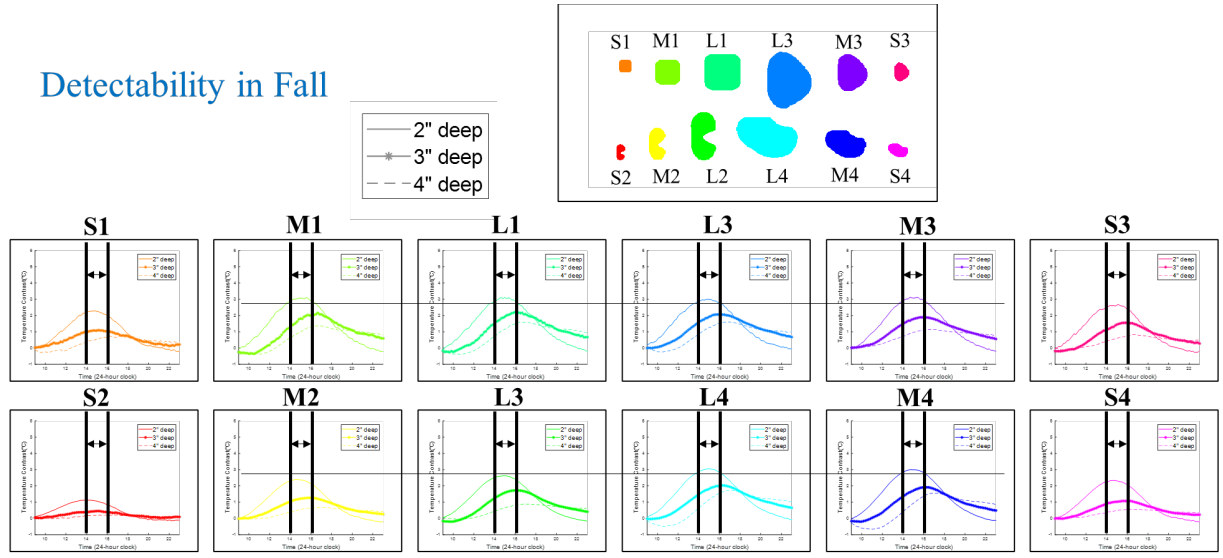

(1) During the optimal time window (**14:00 to 16:00**), the smallest (1 sf) and deepest (4 in) delam develops a contrast of 0.5~0.8°C.
(2) In fall, the maximum contrast can reach 3°C for the largest dealm at shallowest depth.
(3) The contrast development is less impacted by size at Fall season (medium and large size delam shows very similar trend to summer's).

Figure19. The summary of all numerical simulation cases during a typical summer day and a typical fall day

3.3. Coring Validation Results

The *CPR* (correct prediction rate), the σ *CPR* (standard deviation of the four *CPR*s), and the estimated *EP* (efficiency performance) are used to measure the field testing results.

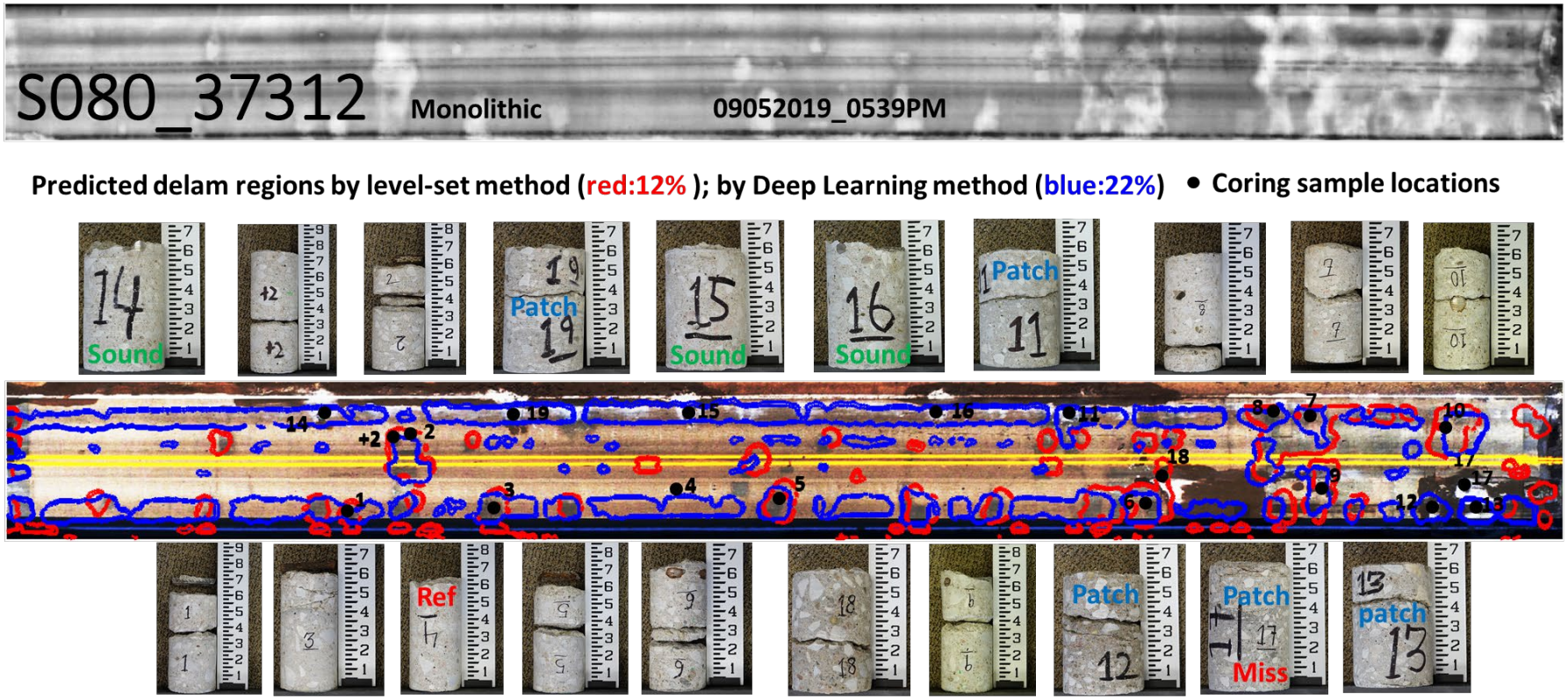

Figure 20. S080_37312 Coring results:
Level-set
CPR_{L1} = 15/20 X100% = 75% (15 correct, 5 misses, 0 false positive)
Deep Learning
CPR_{D1} = 15/20 X100% = 75% (15 correct, 2 misses, 3 false positive)

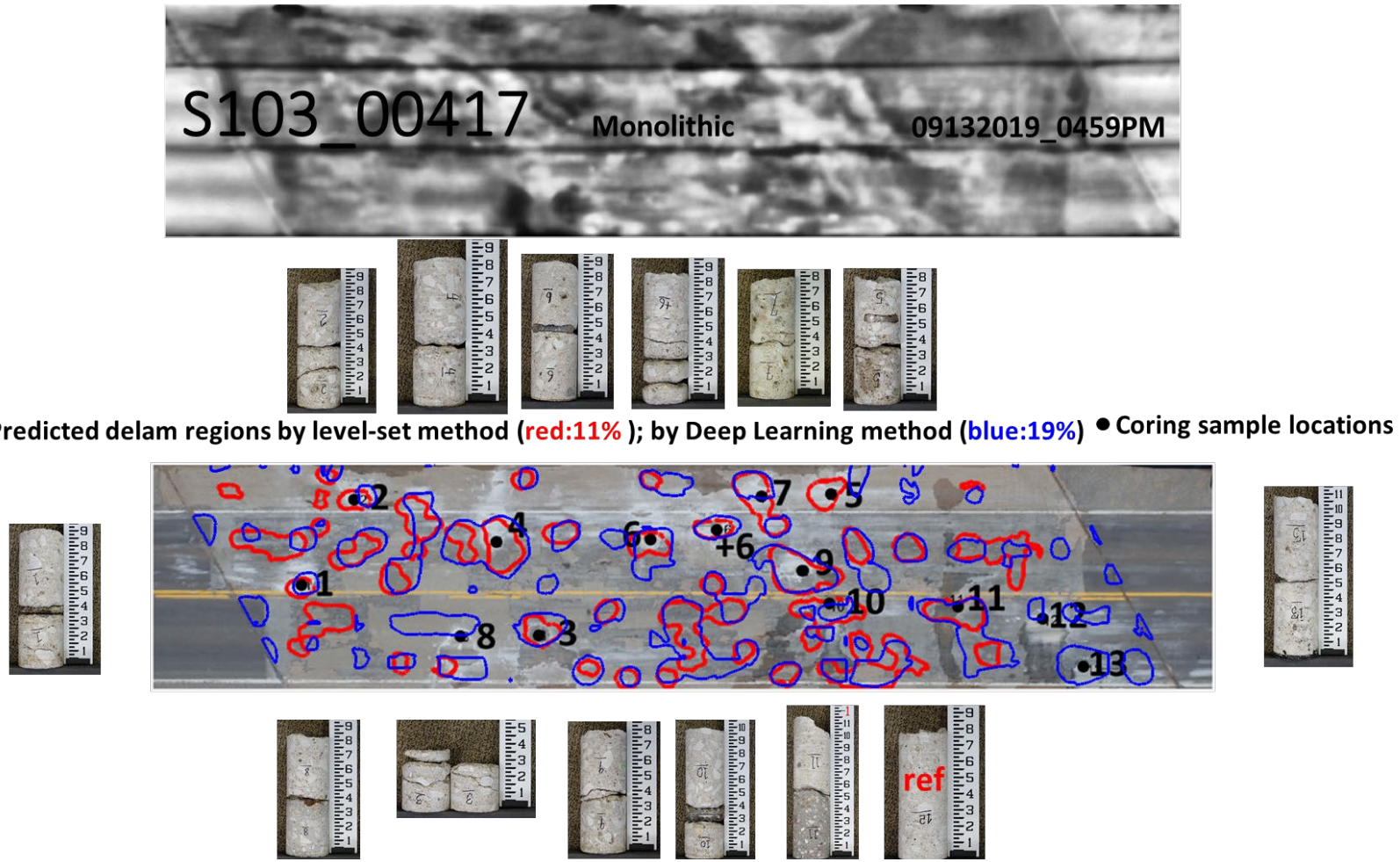

Figure 21. S103_00417 Coring results:
Level-set
CPR_{L2} = 11/14 X100% = 79% (11 correct, 3 misses, 0 false positive)
Deep Learning
CPR_{D2} = 13/14 X100% = 93% (14 correct, 1 miss, 0 false positive)

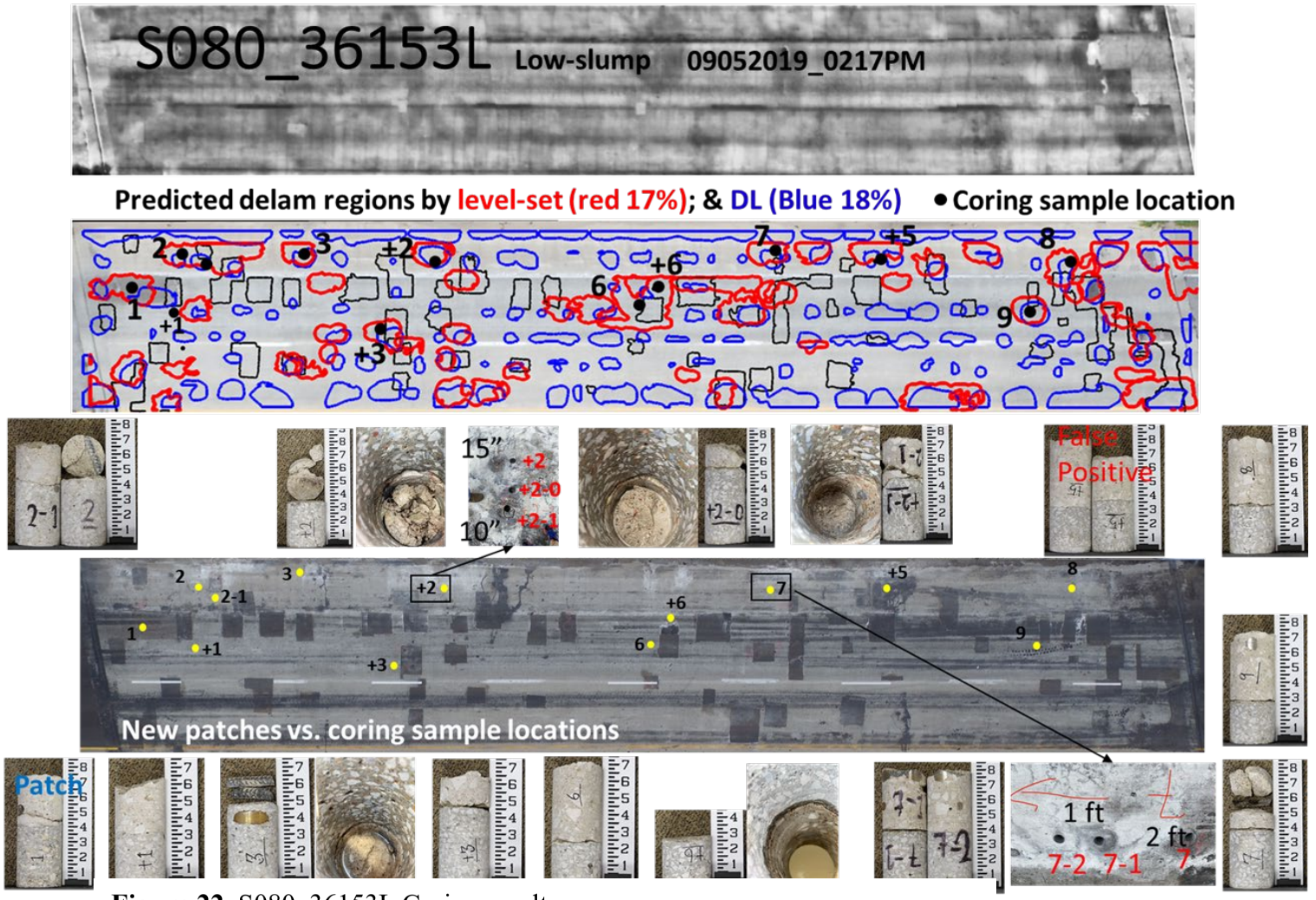

Figure 22. S080_36153L Coring results:

Level-set

CPR_{L3} = 11/13 X100% = 85% (11 correct, 0 misses, 2 false positive)

Deep Learning

CPR_{L3} = 10/13 X100% = 77% (10 correct, 3 misses, 0 false positive

Chain dragging

CPR_{C3}= 2/13 X100% = 15% (2 correct, 11 misses, 0 false positive

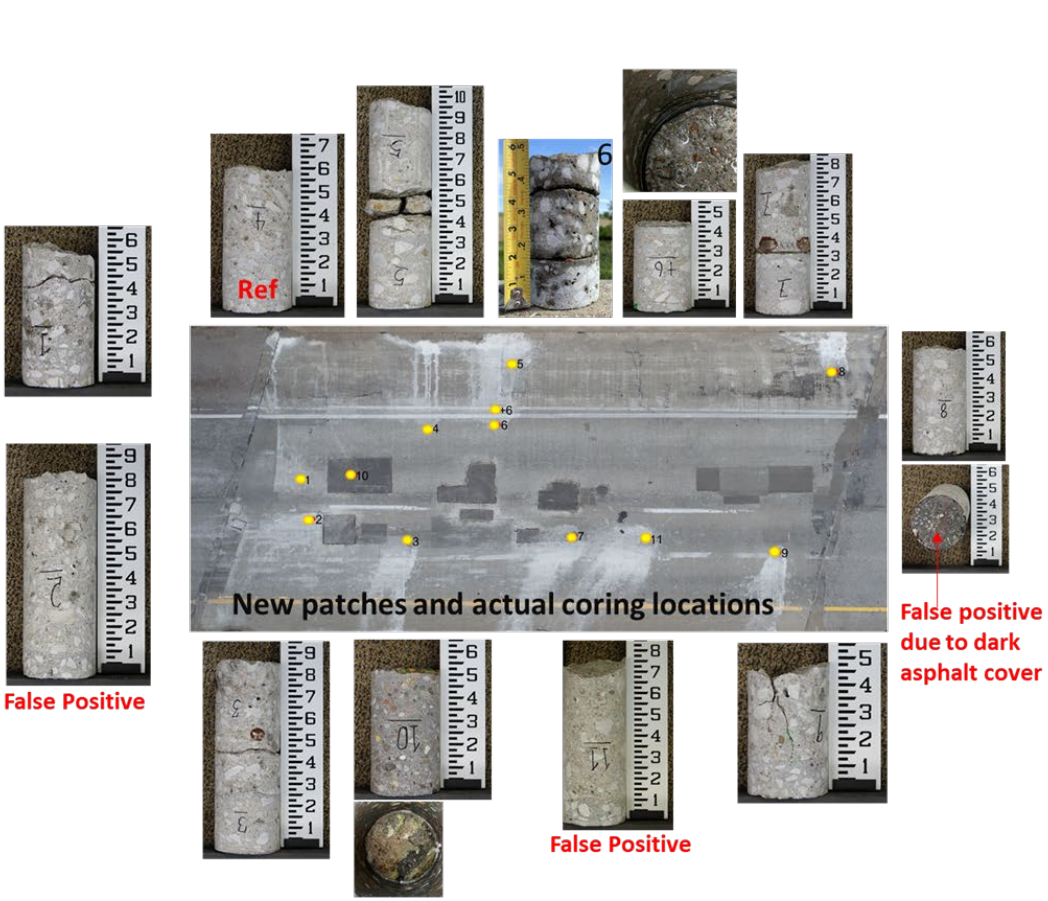

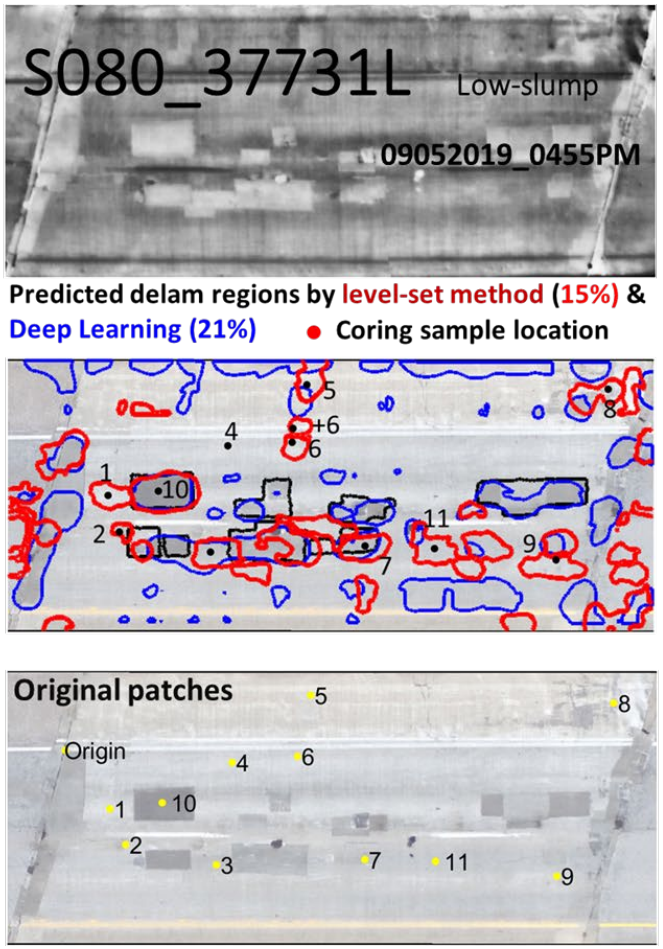

Figure 23. S080_37731L Coring results:
Level-set
CPR_{L4} = 9/12 X100% = 75% (9 correct, 0 misses, 3 false positive)
Deep Learning
CPR_{C4} = 8/12 X100% = 67% (8 correct, 4 misses, 0 false positive)

In summary, the level-set method has an average of 80.2% *CPR* (correct prediction rate); and the deep learning method achieved 78% CPR. The only chain dragging outcome came from bridge S080_36153L, where the CPR is 15%. σ CPR (standard deviation of the four CPRs) of the level-set method is 7.0%; σ CPR of the deep learning method is 9.4%. The low σ CPRs of both developed methods indicated their relatively consistent and robust performance in detecting concrete delamination. It appears that the σ CPR of the deep learning method is slightly greater than the level set method, which indicated that performance of the deep learning method was less consistent (large variance) than the level-set method.

When compared the level-set predicted delamination regions to the chain dragging regions using the new patches as shown in Figure 22, it is very clear that there is a large discrepancy. It appears more than 50% of the new patches were in the good areas predicated by the level-set method. In the meantime, more than 50 % of the level-set predicted delamination regions were not repaired. The coring outcomes indicated an 92% CPR of the level-set method and 77% CPR of the deep learning method on this bridge deck.

4. Conclusions and Limitations

4.1 Conclusions

We finished the project with the following conclusions: (1) The project results suggested that IRT technology could be a complementary method for evaluation of delamination in concrete bridge decks in addition to the existing chain dragging method currently used by NDOT. (2) The new IRT method showed satisfactory performance in accuracy, efficiency, detection depth, and safety. (3) The supervised deep learning framework showed comparable performance to the level-set method though more experiments and training data are needed to assess its robustness. (4) The simulation outcomes suggested the best observation windows for IRT are from 2:00 PM to 4:00 PM in spring and fall, and from 2:00 pm to 5:00 pm in summer. All the time mentioned above are based on the local summer daylight saving time.

Implementation considerations

The research outcomes and conclusions are primarily based on the IRT data collected by the FLIR A8300sc camera system.

Both recording and exporting thermal data using the FLIR 8300sc camera system need to use FLIR's proprietary software ResearchIR Max. MATLAB can process the temperature data from ResearchIR as FLIR-tiff file format. Therefore, for future implementation of the developed technology using similar high-performance cameras, personnel with knowledge of ResearchIR Max is preferred for data acquisition.

Limited experiment using DJI Zenmuse XT thermal camera (FLIR sensor) was conducted on a south Lincoln bridge on US 77. Using the same image processing technology to process the XT thermal image generated slightly different but comparable result. More data collected by the XT cameras are needed to implement the developed technology using the XT camera in the next phase.

The price tag of the XT camera is about $1/10^{th}$ of the price tag of FLIR 8300sc camera. The XT camera records temperature image data in a Radiometric JPEG (R-jpeg) format in the camera's data storage card. The thermal data recording and exportation do not rely on FLIR ResearchIR software. An implementation starting with DJI XT series cameras seems a reasonable choice for a pilot implementation program.

The developed DelamKing prototype was designed to process both FLIR-tiff file format or FLIR R-jpeg file format for future NDOT implementations.

4.2 Limitations

Despite many significant advantages, there are notable limitations when applying the technology in the field. The limitations come from the fact that the developed technology relies on the dissimilarity of deck surface temperatures when the decks are under the same solar-heating and

environmental conditions. There are other environmental conditions or heating sources that can also cause the temperature dissimilarity among different regions on the deck surface. Without proper contextual information, the developed technology is not always able to correctly predict the delaminated areas. Therefore, the performance of the detectability of the developed technology is sensitive to environmental conditions.

In addition to choosing the right time windows, there are some common pitfalls that need to avoid during surveying are: 1) lasting shadows from trees, bridge parapet walls, light poles etc.; 2) dark asphalt smears on concrete decks; 3) excessive dirt/gravel coverings on the deck surface; 4) patches of significantly different materials/colors and textures; and 5) wet deck surfaces, or even dry surfaces shortly after rains. The list can go on, and the users' discretion and filed experience are needed before processing the image data.

5. Best Practice and Recommendations

5.1 Camera and Drone Selection

Two types of cameras (RGB and thermal) are required for data collection. Table 3 lists the recommended specifications for the typical RGB and thermal cameras. For RGB camera, a resolution higher than 4K is suggested. Because with this level's resolution, the camera can capture a bridge less than 340 feet in a single image and return 1 inch per pixel resolution. For the Infrared camera, the wavelength in mid- (3-5μm) and long-range (8-14 μm) are both suitable for the task. In general, a high-end infrared camera (FLIR A8300) has 1K resolution while the medium-level infrared camera (DJI XT) has a 0.5K resolution.

Table 3. Image resolution recommendations

Camera	Recommendation
RGB	Resolution >= 4K, the higher resolution the better
Infrared (Thermal)	Mid-wave(3-5μm) or Long-wave (8-14 μm), the higher resolution the better

Depending on the selected camera, the choice of drones can be determined based on the allowable payload. In this project, two configurations of camera and drone combination are used. Table 4 lists the current and alternative combinations. In general, the RGB camera is light and thus, can be mounted in most drones. The Infrared camera, such as FLIR A8300, has a weight of over 10 pounds, which requires a big drone to handle the payload. Alternatively, some uncooled infrared cameras, such as the DJI XT, is a lightweight infrared camera and can be mounted on the same drone where the RGB camera is mounted. Recently, DJI and FLIR produced an integrated camera system that combines RGB and infrared cameras, DJI XT2, which can collect RGB and Infrared data simultaneously. Both DJI XT and XT2 can be considered as a candidate for delamination detections.

Table 4. Drone and camera recommendations

Case	Combination Recommendation
1	DJI X5 (RGB camera) + DJI inspire one (drone) FLIR A8300 (Infrared camera) + DJI Matrice 600
2	DJI XT (Infrared camera) and DJI X5 (RGB camera) + DJI inspire 1 (drone);
3	DJI XT2 (Infrared and RGB camera integrated) + DJI inspire 2 (drone);

5.2 Field Survey Planning

Before each trip, the schedule for workload, flight path, flight speed, and flight height need to be planned and the focus on equipment checking is recommended. To have efficient and safe data collection, two scenarios are discussed for capturing single image and multiple images at conditions of low and high traffic volume.

a. *Workload estimation (efficiency)*. The workload estimation aims to determine how many bridges can be surveyed at one trip within the optimal time window. To estimate the workload, the survey efficiency is derived based on the field survey operation (Figure 26). This efficiency is estimated based on the experience gained in this project, which can be seen in Figure 5. In general, within the optimal time window (see 5.8 for detail), 3 to 5 bridges can be planned for a one-day trip. The factors that affect the survey efficiency are the length of bridge span, traffic volume, and travelling between bridges.

b. *Flight path.* Figure 24 shows the recommended path schedules in four conditions. The drone is recommended to take off at a flat ground near the bridge (spot 1) and follow the ordered path. For the cases that only require a single shot for entire bridge deck (Figure 24 left), the UAV can hoover at spots 2 and wait for the traffic. For the case requires to collect multiple images (Figure 24 right), the drone is suggested to follow the centerline of the bridge at the low traffic area. For the bridges that have high traffic volume, two trips can be applied to collect the data along the side of the bridge. At the planning stage, the survey mode needs to be planned for each bridge.

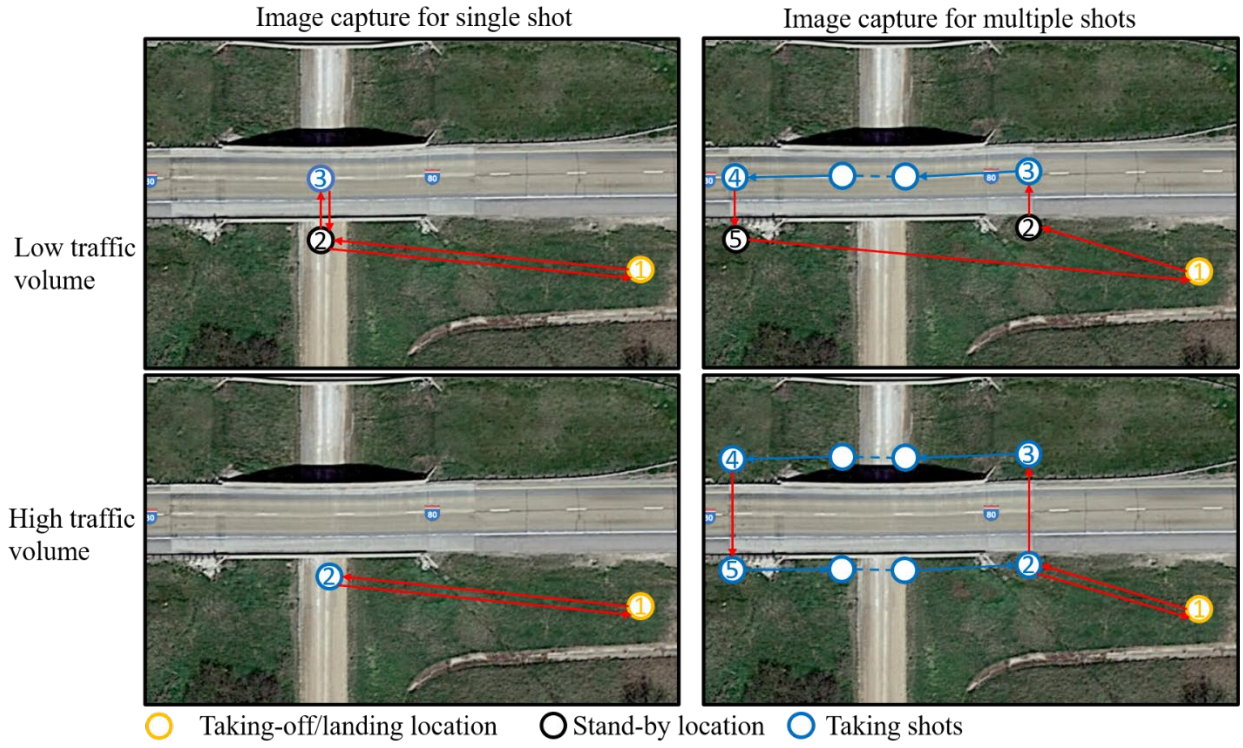

Figure 24. Illustration of flight path for data collection.

c. *Flight Speed.* Since the flight path is simple and straight-forward, manual UAV control is recommended. The flight speed is suggested from 1 to 2 meters per second. Under this speed, the drone can scan a typical bridge (e.g., 300 feet span) within a minute.

d. *Flight height.* The flight height is determined by the bridge geometry (length and width) and the image capture mode (see Figure 25 for illustration). It is suggested when capturing the entire bridge in a single image, the flight height is estimated to cover just the bridge span (shown in Figure 27). For capturing multiple images by the thermal camera (FLIR A8300 with 25 mm lens), the typical flight height is about 50 meters (164 feet) above the ground to cover a 3-lane width bridge. For wider bridges, such as bridges with 4-lane width, a flight height of about 70 meters (230 feet) is recommended.

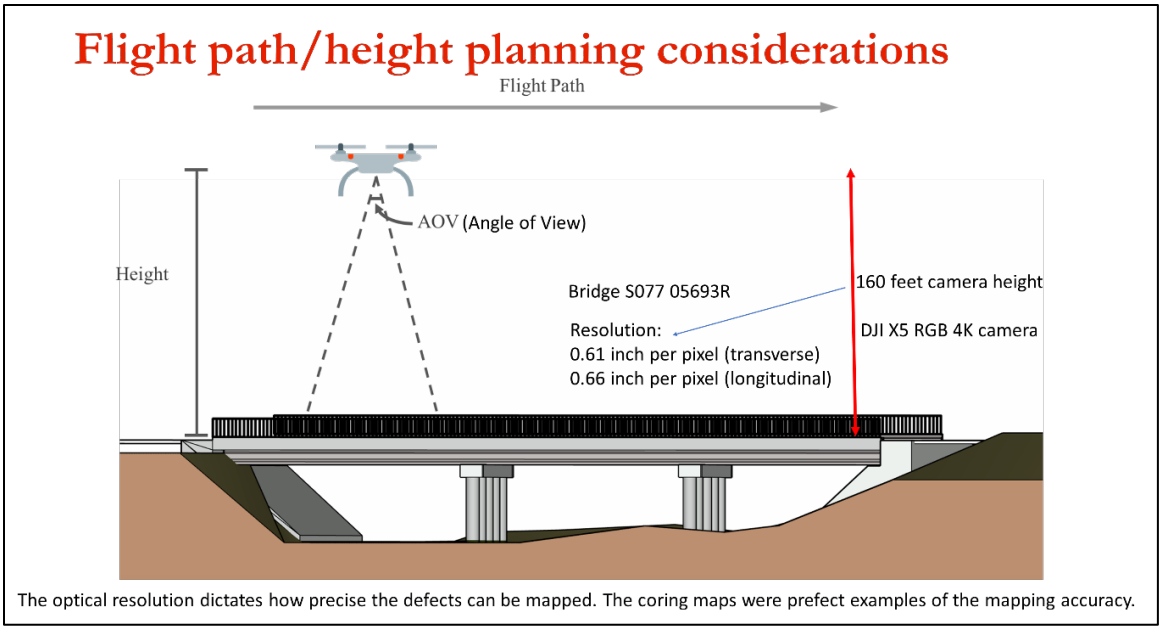

Figure 25. Drone flight height and resolution considerations

e. *Equipment checking.* The focus of checking is on the UAV part, camera, and battery. The UAV is recommended to follow the general routine of maintenance by the manufactory. Other examination on the wear of landing gear, propeller, and motors are recommended before each trip. Cleaning the camera lens is also a key step to ensure the quality of captured data since it often gets dirty after the field survey. Making sure the UAV battery is fully charged and sufficient for the planned workload. For example, based on the UAV system used in this project, one-battery per one-flight for a long bridge (such as a span large than 200 feet) is recommended. One-battery per two-flight for a short bridge (less than 200 feet) is workable in low wind conditions (< 10mph). When on high wind conditions (10 mph to 15 mph), one-battery per one-flight is suggested.

5.3 Field Operations

Based on current practice, the survey operation consists of three steps: pre-survey, at-survey, and after-survey.

a. *Pre-survey.* When arriving at site (pre-survey), a flat ground for UAV taking off and landing needs to be selected. Once UAV is setup, taking off the UAV and hoover at spot

1 (in Figure 24) for several seconds. During the hoovering, checking any warning message from the control screen and observing any irregular behavior of the UAV. This step normally takes 15 to 30 minutes.

b. *At-survey*. Once the UAV works appropriately, the survey can be conducted by following the planned path in Figure24. Based on current practice, using a smaller drone to capture RGB image for the first flight is suggested. Because the small drone with light weight payload can be easier controlled compared to heavy-loaded large drone, if unexpected situation happens (such as signal interference during flight). Then, the second flight for thermal image capture can be followed. This step normally takes 15 to 30 minutes.

c. *After-survey*. When all data are collected, checking data quality immediately is recommended. The recommendation of data quality is discussed in data acquisition in section 5.4. This step normally takes up 15 to 30 minutes.

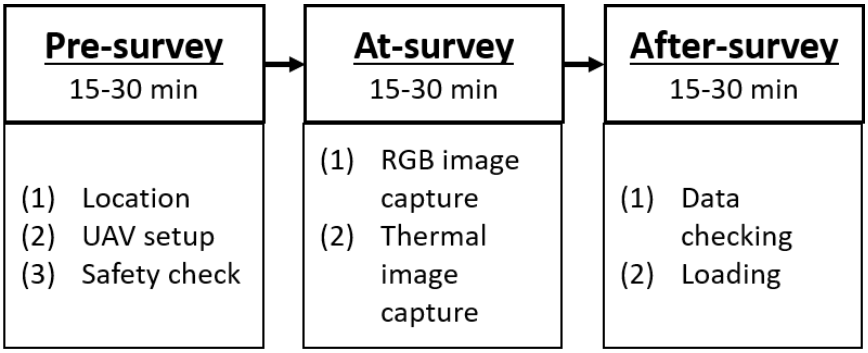

Figure 26. Field survey operation and survey efficiency

5.4 Data acquisition

During the data collection, there are several recommendations for camera setups and image capture:

a. *Camera angle*. For both RGB and Infrared images, the camera needs to face perpendicular downward to the ground. This provides the best image quality for later image processing.

b. *Image coverage*. Depending on the image capture mode, figure 27 illustrates the recommended coverage for each image. Figure 27a Figure 26a shows an example when the entire bridge deck can be covered in the single shot mode. Figure 27b shows that when using multiple shots mode, leaving extra space on both sides of the bridge is suggested. This reserved space is helpful to reduce the impact from flight instability and thus, improve the image registration accuracy in the later process.

c. *Sampling rate*. For multiple shots mode, the sampling rate for the thermal camera (FLIR A8300 in the project) is recommended about 3 Hz to 5 Hz. Under this rate, the overlap between images can be over 80% and the overlap is sufficient for later image registration.

d. *Data format.* When using DJI XT Infrared camera, the image needs to be set as R-jpg (radiometric jpg) and save as TIFF format. In this setup, the captured thermal image can be used for later analysis by the developed method.

e. *Shadow impact*. Try to collect data at a right time to avoid shadow's impact. The shadow caused by surrounding trees and parapet will negatively affect the detectability of the developed segmentation algorithms. Based on the observation in surveyed bridges, it was found that most of the shadow often came from the parapet walls. Thus, collecting data at a right time for differently orientated bridges is useful to address the issue. For example, the best time to collect data for a north-south oriented bridge is midday.

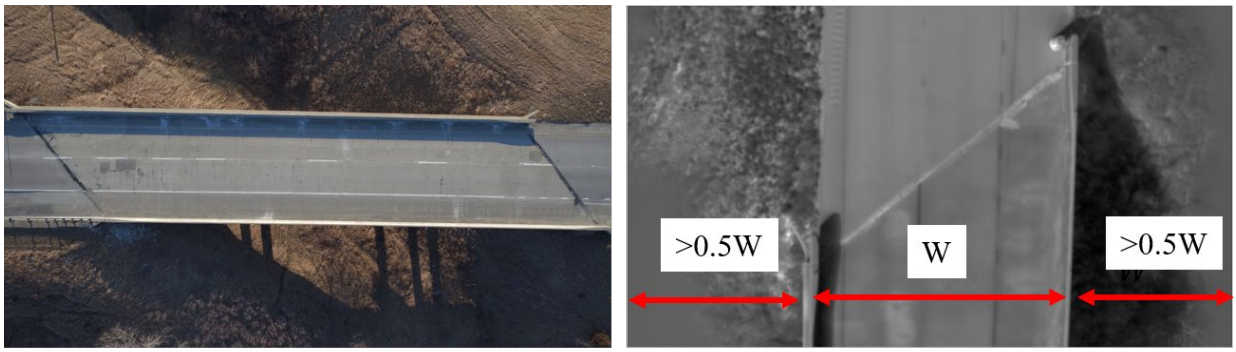

(a) Capture entire bridge at single shot (b) Capture part of bridge

Figure 27. Illustration of image coverage for (a) single shot mode and (b) multiple shots mode.

5.5 Survey Crew

In the best practice of safety and efficiency, three crew members are desired for the team. The members play three key roles: UAV operation, visual observation of UAV, and traffic observation. During the flight, the UAV operator can focus on the flight by navigating using the camera view. The visual observer is then responsible to monitor the UAV's behavior and maintain the UAV's visual line of sight (VLOS). Notify any irregularity of the UAV to the operator. The traffic observation is responsible for monitoring the traffic flow and notify the operator of any incoming traffics.

5.6 Safety Considerations

To ensure a safe survey, several key considerations are suggested:

a. *UAV check*. The drone needs to be checked before each trip. The propeller, motor and screws in the component experienced high vibration need additional attentions.

b. *Landing location*. During the data collection, the take-off/landing location needs to be a flat ground. If no flat ground is available, a portable landing platform is needed. Taking off or landing on a very sloped surface could result in over-turn of the drone.

c. *Radio signal interference*. Before drone taking off, the magnetic and wireless signal interference need to be checked. Radios of passing-by trucks or power lines may generate interrupting strong signals.

d. *Powerline/tree obstacles*. Try to avoid taking off or landing close to a power lines or trees.

e. *Emergency*. An emergency landing area needs to be planned in case of losing control of the drone.

5.7 Weather Condition

To ensure operational safety and data quality, the following weather conditions are suggested:

a. On the day of data collection, a sunny condition is required. No precipitation for several days before the survey is desired since the water may be trapped in the delamination and degrade the detectability in the thermal image.

b. Wind speed under 10 mph is favored for a smooth flight. Wind speed higher than 15 mph will cause instability for drone operation (especially carrying heavy payload). Windy day (> 15 mph) with high gust is not recommended for data collection.

c. The favorable season for data collection is summer and early fall based on current experience. Late fall and winter seasons are not recommended for data collection due to the battery performance degradation in cold weather.

5.8 Survey Time Windows

Based on experimental and numerical studies in this project, the following time window is recommended to ensure data quality:

a. In typical summer days, the best time window is from 2 P.M. to 5 P.M.

b. In typical spring and fall days, the best time window is from 2 P.M. to 4 P.M.

5.9 Data Flow

Figure 28 demonstrates the data captured from cameras to the final delamination quantification. At the stage of data acquisition, the RGB camera, such as DJI X5, captures an image of a bridge deck and saves it as a jpg file in the internal storage. The infrared camera, such as FLIR A8300, collects the raw data to the on-board computer and then converts the data to TIFF files through *ResearchIR* software. Then the image data is transferred to a PC for post processing. At the stage of data processing, the jpg and TIFF files are processed by MATLAB software through customized functions. At the final stage, the result is exported in a form of delamination profiles mapped on RGB images with the quantification of area percentage.

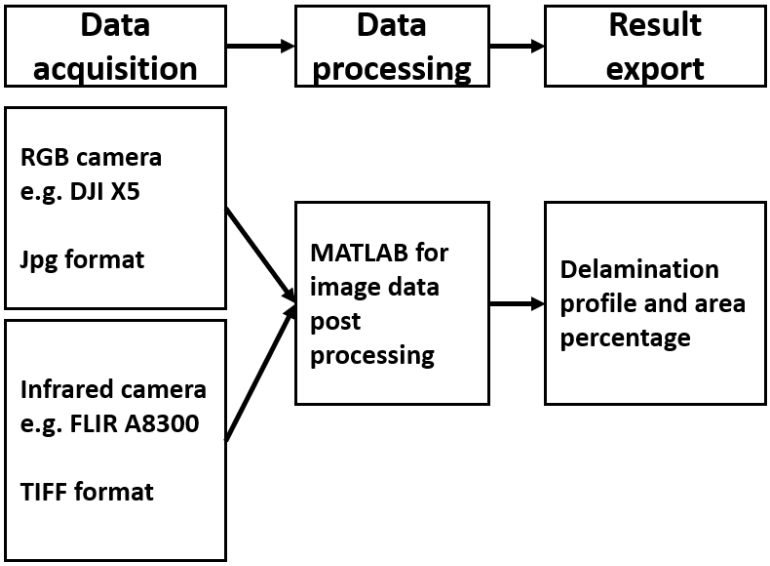

Figure 28. Data flow

5.10 Post Processing of Image Data

To have the delamination quantification, the raw data collected from RGB and infrared cameras are suggested to be transferred to a PC for further processing. Figure 28 shows a proposed procedure for image data post processing. The RGB and thermal image are processed through a series of steps (horizontal alignment, crop, stitching, and registration) and finally achieve a pixel-level coordinate correspondence. Then, the image is rescaled to a recommended resolution of 1 inch per pixel. The level-set processing module then takes the thermal image as input and returns the delamination profiles (pixel-level localization). In the module of result export, the delamination detected from the thermal image is mapped on the RGB image and the area percentage will be calculated.

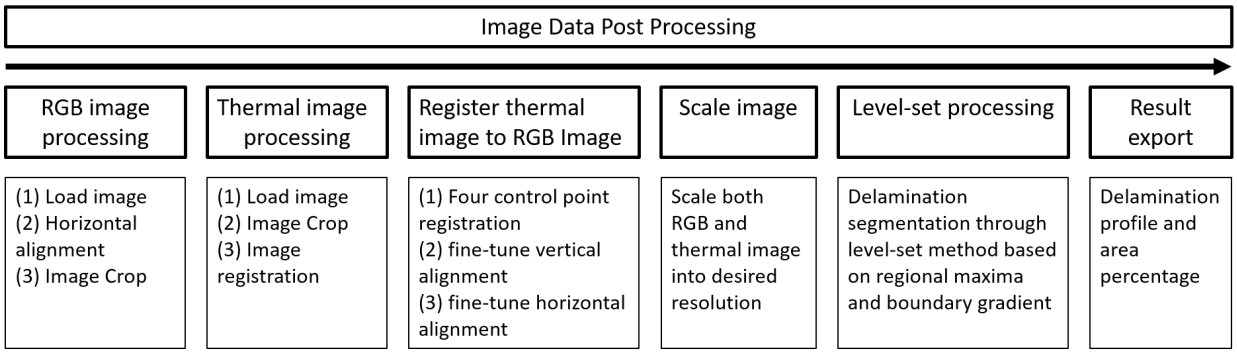

Figure 29. Image data post processing

References

1. Iowa DOT (1982). "Bridge deck delamination study infrared inspection", IADOT HR-244, http://publications.iowa.gov/19643/1/IADOT_hr244_Detection_Concrete_Delamination_Infrared_Thermography_1986.pdf

2. WSDOT (2008). "Detection of Voids in prestressed concrete bridges using thermal imaging and GPR". https://www.wsdot.wa.gov/research/reports/fullreports/717.1.pdf

3. Iowa DOT (2012). "I-129 Missouri River Bridge Deck Condition Assessment Using Non-Destructive Testing Methods" https://www.iowadot.gov/research/reports/Year/2012/fullreports/I-129%20Deck%20Condition%20Assessment%20Final%2011%205%2012.pdf

4. Iowa DOT (2013). "Evaluation of Hand-Held Infrared Cameras for Bridge Deck Inspection". SP&R RB15-012, https://iowadot.gov/research/reports/Year/2013/fullreports/Hand-held%20Infrared%20Camera%20Evaluation.pdf

5. NDDOT (2017). " Using infrared thermography for NDE of bridges" https://www.dot.nd.gov/conferences/opd/OPD/IRThermographyBridgeEval.pdf

6. Vaghefi, K., T. M. Ahlborn, D. K. Harris, and C. N. Brooks. (2013) "Combined imaging technologies for concrete bridge deck condition assessment. Journal of Performance of Constructed Facilities, 29(4). p. 04014102.

7. P. Cotič et al. (2015). "Determination of the applicability and limits of void and delamination detection in concrete structures using infrared thermography". NDT&E International 74 (), 87–93

8. Hiasa, S., R. Birgul, and F. N. Catbas. (2017) "Investigation of effective utilization of infrared thermography (IRT) through advanced finite element modeling". Construction and Building Materials, 150(), 295-309.

9. Hiasa, S., F. Necati Catbas, M. Matsumoto, and K. Mitani.(2017). "Considerations and issues in the utilization of infrared thermography for concrete bridge inspection at normal driving speeds." *Journal of Bridge Engineering*, 22(11), p. 04017101

10. Cheng, C., and Z. Shen. (2018). "Time-Series Based Thermography on Concrete Block Void Detection". Construction Research Congress 2018. pp. 732-742.

11. Cheng, C., Shang, Z., and Shen, Z. (2019) "Enhancing Bridge Deck Delamination Detection Based on Aerial Thermography through Grayscale Morphologic Reconstruction: A Case Study", TRB-2019 Annual Meeting, Jan. 13-17, Washington D.C.

12. Cheng, C., and Shen, Z. (2020). "Semi Real-time Detection of Subsurface Consolidation Defects during Concrete Curing Stage", *J. of Construction and Building Materials.121489.*

13. Cheng, C., Shang, Z., and Shen, Z. (2019) "Bridge deck delamination segmentation based on aerial thermography through regularized grayscale morphological reconstruction and gradient statistics", *J. of Infrared Physics & Technology,* 98(), 240-249

14. Cheng, C., and Shen, Z. (2020). “The application of level-set method in segmentation of concrete deck delamination using infrared images”, *J. of Construction and Building Materials* (240) 117974

15. Cheng, C., Shang, Z., and Shen, Z. (2020). “Automatic Delamination Segmentation for Bridge Deck Based on Encoder-Decoder Deep Learning Through UAV-based Thermography”, 116: 102341, *J. of NDT & E International*

16. Cheng, C., Na, R., and Shen, Z. (2019). “Thermographic Laplacian-Pyramid Filtering to Enhance Delamination Detection in Concrete Structure”, *J. of Infrared Physics & Technology,* 97(), 162-176